

The apparent 2D metal-insulator transition as a strong localization induced crossover phenomenon: Implications from the Ioffe-Regel criterion

S. Das Sarma¹ and E. H. Hwang^{1,2}

¹*Condensed Matter Theory Center, Department of Physics,
University of Maryland, College Park, Maryland 20742-4111*

²*SKKU Advanced Institute of Nanotechnology and Department of Physics,
Sungkyunkwan University, Suwon, 440-746, Korea*

(Dated: August 6, 2015)

Low-disorder and high-mobility two-dimensional (2D) electron (or hole) systems confined in semiconductor heterostructures undergo an apparent metal-insulator-transition (MIT) at low temperatures as the carrier density (n) is varied. In some situations, the 2D MIT can be caused at a fixed low carrier density by changing an externally applied in-plane magnetic field parallel to the 2D layer. The goal of the current work is to obtain the critical density (n_c) for the 2D MIT with the system being an effective metal (Anderson insulator) for density n above (below) n_c . We study the 2D MIT phenomenon theoretically as a possible strong localization induced crossover process controlled by the Ioffe-Regel criterion, $k_F l = 1$, where $k_F(n)$ is the 2D Fermi wave vector and $l(n)$ is the disorder-limited quantum mean free path on the metallic side. Calculating the quantum mean free path in the effective metallic phase from a realistic Boltzmann transport theory including disorder scattering effects, we solve the integral equation (with l depending on n through multidimensional integrals) defined by the Ioffe-Regel criterion to obtain the nonuniversal critical density n_c as a function of the applicable physical experimental parameters including disorder strength, in-plane magnetic field, spin and valley degeneracy, background dielectric constant and carrier effective mass, and temperature. The key physics underlying the nonuniversal parameter dependence of the critical density is the density dependence of the screened Coulomb disorder. Our calculated results for the crossover critical density n_c appear to be in qualitative and semi-quantitative agreement with the available experimental data in different 2D semiconductor systems lending credence to the possibility that the apparent 2D MIT signals the onset of the strong localization crossover in disordered 2D systems. We also compare the calculated critical density obtained from the Ioffe-Regel criterion with that obtained from a classical percolation theory, concluding that experiments support the Ioffe-Regel criterion for the 2D MIT crossover phenomena.

I. INTRODUCTION

Carrier transport in 2D semiconductor structures [e.g., Si inversion layers in MOSFETs, 2D electron gas (2DEG) or 2D hole gas (2DHG) GaAs-AlGaAs heterojunctions and quantum wells or in Si-SiGe quantum wells] is a strong function of carrier density (n) and temperature (T)¹⁻⁶. The study of 2D electronic (which include holes also in 2D p-doped structures) transport at low temperatures divides itself naturally into two distinct areas: effectively “metallic” transport at high carrier density manifesting a weak or moderately positive $d\rho/dT \gtrsim 0$ and effective insulating temperature dependence at low carrier density manifesting a large negative $d\rho/dT < 0$ at low temperatures, where $\rho(T)$ is the temperature dependent 2D resistivity. The current work aims at a theoretical understanding of the density-tuned crossover behavior between this high-density effective metallic and the low-density effectively insulating transport behavior at low-temperatures. Consistent with the widely used terminology, we refer to this density tuned low-temperature phenomenon (i.e., a change of sign in $d\rho/dT$) as the 2D metal-insulator transition (“2D MIT”), but it is more likely to be a crossover behavior rather than an actual quantum phase transition, and indeed in the current work we treat the 2D MIT phenomenon manifestly as a crossover behavior (as already made explicit in the ti-

tle of this paper) characterized by the Ioffe-Regel criterion. We emphasize right here in the beginning that ours is not a critical theory for a quantum phase transition. This is also highlighted in the title of our paper through the words “apparent” and “crossover”. We also emphasize that our current work is not a theory for the temperature-dependent transport properties of the metallic or the insulating phase, which have been much studied in the literature, but is a theory for the transition density itself, which has not been studied at all in the theoretical literature.

Prior to 1979 – 80, when the scaling theory of localization⁷ came into being, the 2D MIT phenomenon in Si inversion layers (based on Si-SiO₂ MOSFET structures) was universally considered to be an example of the Anderson localization transition^{1,8,9}, where decreasing 2D carrier density drives the system from being a 2D metal at high density to being a 2D insulator at lower density as the Fermi level moves through a mobility edge. The scaling theory of localization⁷ established two to be the lower critical dimensionality in the non-interacting localization problem, and thus all disordered 2D electronic states are now (i.e., after 1979) thought to be strictly localized although the localization length is exponentially long for weak disorder, making it essentially impossible to distinguish a true extended metallic state from a weakly localized insulating state in finite

samples (or at finite temperatures) with the localization length exceeding the sample size (or the temperature-dependent inelastic phase breaking length). For high disorder, however, the 2D system becomes exponentially localized (“strong localization”) and the crossover from “weak localization” (which is a logarithmically weak effect) to “strong localization” (which is exponential localization with the single-particle wavefunction falling off exponentially with distance in contrast to weak localization with exponentially long localization length) is the subject matter of the current work. With no loss of generality, the weakly localized higher-density phase will be referred to as the “metallic” phase in this paper and the lower density strongly localized phase will be referred to as the “insulating” phase. Experimentally, the two phases (i.e., high-density weakly-localized or “metallic” and low-density strongly localized or “insulating”) are distinguishable by the temperature dependence of their respective low-temperature resistivity with the strongly localized low-density phase manifesting the exponential insulating behavior with a strongly exponentially increasing resistivity with decreasing temperature whereas the metallic high-density phase either exhibiting almost no temperature dependence in its resistivity (at very high density) or the resistivity decreasing (as an effective power law) with decreasing temperature (at not very high density). In principle, the “metallic” phase should manifest a weak logarithmic insulating temperature dependence of low enough temperatures because of the weak localization property of the 2D metallic phase as predicted by the scaling theory, but the observation of such a weak logarithmic insulating temperature dependence is challenging since it is easily overwhelmed by any other power-law temperature dependence in the system (except perhaps at extremely low temperatures) arising, for example, from phonon or screening effects. At very low temperatures, the logarithmic insulating temperature dependence should dominate even in high-density samples, but such low electronic temperatures are often impossible to reach because of carrier heating problems invariably present in semiconductors. We ignore the 2D weak localization complications^{10,11} in the rest of this paper, referring to the higher-density phase as an effective 2D metal (and the lower-density strongly localized phase as a 2D insulator).

In this paper we theoretically study the weak to strong localization transition (or the apparent transition from the effective metal to the effective insulator) as a function of carrier density at a fixed low temperature. It is expected that this transition, which is technically a crossover, happens around $k_F l = 1$ as defined by the so-called Ioffe-Regel criterion, where k_F is the 2D Fermi wave vector and ‘ l ’ is the disorder-induced elastic quantum mean free path. We note that $k_F \propto \sqrt{n}$ in 2D systems, but ‘ l ’ itself is a complicated functional of ‘ n ’ defined through a complex integral function $l(n)$. Thus, the condition $k_F l = 1$ would define an effective crossover “critical density” n_c with $n > n_c$ being the 2D metallic

phase (where $l > k_F^{-1}$) and $n < n_c$ being the (strongly localized) 2D insulating phase (where $l < k_F^{-1}$ in our theory). We emphasize that the $n > n_c$ metallic phase is only an effective metal in finite samples.

In addition to obtaining the qualitative dependence of the crossover density n_c for 2D MIT as implied by the Ioffe-Regel criterion on the 2D materials parameters (e.g., effective mass, valley degeneracy, dielectric constant,, etc.), our main goal would be to ascertain the qualitative dependence of n_c on disorder. Since disorder determines the mean free path ‘ l ’, the crossover ‘critical’ density n_c , as obtained from the condition $k_F l = 1$, would depend crucially on disorder parameters. More disordered the system, the higher would be n_c since the effective mean free path would be smaller for larger disorder. Since the effective disorder (and therefore the mean free path itself) is temperature dependent, n_c would manifest an implicit temperature dependence through the temperature dependence of the 2D metallic conductivity, which we would also study theoretically although, strictly speaking, n_c is defined only at $T = 0$ which is indeed the focus of our theory. Another aspect of experimental interest we study theoretically in this paper is the effect of a parallel magnetic field which tends to spin-polarize the system leading to suppressed screening and hence enhanced effective disorder (and thus a suppressed metallic conductivity and a reduced mean free path). Thus, an in-plane applied magnetic field increases n_c (since it decreases the effective mean free path) consistent with experimental observations. The dependence of the crossover critical density n_c on disorder and magnetic field is the focus of our current theoretical work, where we uncritically use the Ioffe-Regel criterion to define the metal-to-insulator apparent transition. We emphasize that this work is not a theory describing the properties of either the higher-density ($n > n_c$) apparent metallic or the lower-density ($n < n_c$) insulating phase. These phases have already been studied extensively in the literature over the last 20 years^{1–6}, and we have little to add to these discussions in the current work which is focused entirely on describing the properties of the crossover critical density (i.e., n_c) itself using the Ioffe-Regel criterion as the underlying theoretical principle.

It is important to emphasize that our work is purely phenomenological in nature where the Ioffe-Regel criterion, $k_F l = 1$, plays the central role in determining the crossover density for 2D MIT. Whether this specific description for 2D MIT is valid or not can only be decided *a posteriori* by comparing between our calculated theoretical results for n_c and the corresponding experimental results. We should mention right now that our calculated n_c appears to be in reasonable qualitative and semi-quantitative agreement with the available experimental results (as would later be discussed in this article) on 2D MIT in the literature although detailed quantitative comparisons are difficult since independent experimental information on the applicable disorder in the relevant 2D systems is unavailable. We assume in this work

that the dominant disorder in the semiconductor structures undergoing 2D MIT arises from uncorrelated random quenched charged impurities in the environment¹². There is considerable experimental evidence^{1,13–19} that unintentional random charged impurities in the background and at the interface as well as the remote charged donors (e.g., in modulation doped heterostructures and quantum wells) are the main resistive scattering sources in 2D semiconductor systems at low temperatures (and at low carrier densities where 2D MIT occurs). In Si-MOSFETs the short-range disorder associated with Si-SiO₂ interface¹ certainly plays a role in resistive scattering at higher carrier density (when the 2D electron gas is pushed very close to the interface by the self-consistent electric field generated by the electrons themselves), but for $n \gtrsim n_c$ the main scattering source is the charged impurity disorder even for Si-MOSFETs provided that n_c is not too large¹². We therefore neglect all disorder mechanisms other than random charged impurities in the system, which we parameterize using only two parameters: n_i and d [a 2D density of charged impurity centers of concentration n_i distributed randomly in a plane a distance ‘ d ’ away from the semiconductor-insulator interface where the 2D carrier system is localized – we assume the charged impurities to be of random positive and negative sign of unit strength (i.e., of magnitude e , the electron charge) with a net charge of zero]. We emphasize that it is straightforward to include in the theory additional (as well as more realistic) types of disorder (e.g., interface roughness, alloy disorder, bulk 3D distribution of random charged impurities) and/or a more general model for charged impurity disorder where some correlations among impurity positions are included in the theory²⁰. We neglect all these non-essential details simply because including them would require many more additional unknown parameters to characterize the system disorder compared with our minimal model of disorder which is characterized by only two parameters n_i and d . Since our minimal model (characterized by only two parameters n_i and d) already captures the essential physics of 2D MIT, we believe that this minimal model should suffice for our theoretical purpose. In addition to providing results for n_c based on the quantum Ioffe-Regel criterion, we also carry out a comparison between the critical densities obtained from the Ioffe-Regel theory and from the classical percolation theory which has sometimes been invoked in describing 2D MIT in the context of long-range Coulomb disorder. A comparison between n_c calculated in these two theories and the experimental n_c should tell us whether 2D MIT is a quantum or classical phenomenon.

The rest of this article is organized as follows. In section II we provide the details for the calculation of the crossover critical density n_c using the Ioffe-Regel criterion, giving the general theory, the analytical results, and all the numerical results for realistic systems. We provide a general discussion of our results in section III, particularly in the context of Ioffe-Regel versus percola-

tion criteria as descriptions for the 2D MIT phenomena. We conclude in section IV with a summary of our results and the discussion of open questions.

II. CALCULATION OF CRITICAL DENSITY

In this section, we apply the Ioffe-Regel criterion

$$k_F l = 1, \quad (1)$$

to calculate the crossover 2D MIT ‘critical’ density n_c as a function of system parameters. We first note an immediate problem arising from the uncritical direct application of Eq. (1) in obtaining the critical density n_c . Interpreting ‘ l ’ as the transport (or conductivity) mean free path we can write

$$l = v_F \tau_t, \quad (2)$$

where v_F and τ_t are respectively the Fermi velocity and the transport relaxation time. Using the well-known Drude-Boltzmann formula for the electrical conductivity σ given by

$$\sigma = n e^2 \tau_t / m, \quad (3)$$

and $k_F = (4\pi n / g_s g_v)^{1/2}$ for the 2D electron gas (with g_s and g_v being respectively the ground state spin- and valley-degeneracy factor) and the definition $v_F = p_F / m = \hbar k_F / m$, we get from Eq. (1) the following condition for the critical conductivity $\sigma_c = \sigma(n_c)$ at the transition

$$\sigma_c = \frac{g_s g_v e^2}{2} \frac{1}{h}. \quad (4)$$

Equation (4), which is precisely equivalent to the Ioffe-Regel criterion of Eq. (1) for a 2D electron system, can also be written as

$$\rho_c \equiv \sigma_c^{-1} = \frac{2}{g_s g_v} \frac{h}{e^2}. \quad (5)$$

Thus, in 2D systems the Ioffe-Regel criterion is precisely equivalent to $\rho_c = h/e^2$ if we take the usual situation of $g_s = 2$ and $g_v = 1$ whereas, for Si(100)-MOSFETs with $g_v = 2$, we get $\rho_c = h/2e^2$. It is interesting to note that the straightforward application of Ioffe-Regel criterion leads to a critical metallic resistivity of only $h/6e^2 \sim 4,400 \Omega$ for the 6-fold valley degenerate Si(111)-MOSFETs which have recently been fabricated using Si-vacuum interfaces²¹.

Such a universal critical resistivity characterizing 2D MIT, with $\rho_c = h/e^2 \approx 25,600 \Omega$ for 2D n-GaAs and p-GaAs and $\rho_c \approx 12,800 \Omega$ for Si(100)-MOSFETs [or $4,400 \Omega$ for Si(111)-MOSFETs], is, however, in quantitative disagreement with experimental observations where the reported critical resistivity for the insulating behavior to manifest itself is certainly not universal in a single

material system (i.e., for a given g_s and g_v) and typically varies between 10,000 Ω and 50,000 Ω in various experimental studies although it is often typically within a factor of two of the resistance quantum h/e^2 , thus indicating that the naive consideration given by the direct application of the Ioffe-Regel criterion defined by Eqs. (4) and (5) is certainly reasonably, but not perfectly, accurate. In fact, the pioneering experimental studies of Kravchenko *et al.*²² found $\rho_c \approx 1.5 h/e^2$ in low-disorder MOSFETs and the older highly disordered MOSFETs¹ typically manifested $\rho_c \approx h/4e^2$ although both classes of systems presumably involved $g_v = 2$ and $g_s = 2$ with the only difference between the two being the level of disorder and the concomitant value of n_c (being around $\sim 10^{11} \text{ cm}^{-2}$ and $\sim 10^{12} \text{ cm}^{-2}$ in two classes of systems, respectively). The measurement temperature used in the experiment is also a complication, particularly since the measured resistivity is typically strongly temperature dependent for $n \approx n_c$. The most recent experimental investigations of 2D MIT in high quality Si(100) MOSFET based and Si-Ge based 2D systems (both should have $g_s = g_v = 2$) manifest $\rho_c \approx 2h/e^2$ and $2h/3e^2$, respectively, in contrast to the canonical value $h/2e^2$ [Eq. (5)] expected on the basis of $g_s = 2$ and $g_v = 2$. In n-2D GaAs systems, $\rho_c \approx h/2e^2$ has been found¹⁵ whereas in 2D p-GaAs, the observed ρ_c seems to vary widely with $\rho_c \approx 2h/e^2$ ¹⁸ and $\rho_c \approx h/2e^2$ ¹⁹ both being reported in contrast to the theoretically expected $\rho_c = h/e^2$ for $g_s = 2, g_v = 1$ 2D systems.

Thus, we have a conundrum in using the Ioffe-Regel criterion with ' l ' interpreted as the transport mean free path since this would lead to a (upto a factor of 2) quantitative inconsistency with the experimentally observed variations in $\rho_c \equiv \rho(n_c)$ at the 2D MIT crossover point. We note that this problem of a non-universal experimental ρ_c for 2D MIT within the same material system (i.e., constant g_s and g_v) in contrast with the universal theoretical ρ_c prediction from the Ioffe-Regel criterion (with ' l ' interpreted as the transport mean free path) cannot be resolved by altering the criterion to a different form such as the Mott-Ioffe-Regel criterion²³ where the transition is defined by $k_F l = \pi$ [rather than $k_F l = 1$ as in the original Ioffe-Regel condition defined by Eq. (1)]. Such a modification will only alter Eq. (5) for ρ_c to $\rho_c = (2/\pi g_s g_v)(h/e^2)$, a different (and smaller) universal critical resistivity for constant values of g_s and g_v which is, of course, still in disagreement with the experimental observations. Our possibility that cannot be ruled out in this context is that the critical resistivity ρ_c at $T = 0$ indeed satisfies the expected resistance quantum value given by Eq. (5), but cannot really be accurately determined from finite temperature crossover measurements. The fact that the experimentally measured ρ_c is almost always within a factor of 2 of the expected value defined by Eq. (5) makes this possibility particularly relevant.

A simple modification of the Ioffe-Regel criterion, where ' l ' is interpreted as the quantum mean free path given by $l = v_F \tau_q$ where τ_q is the quantum single-particle

scattering time (rather than the transport relaxation time τ_t), actually provides a variable critical resistivity since there is no simple relationship connecting the conductivity σ with the quantum scattering time τ_q . Using the identity that impurity scattering induced quantum level broadening Γ is related to τ_q by

$$\Gamma = \hbar/2\tau_q, \quad (6)$$

it is easy to see that the Ioffe-Regel criterion Eq. (1), based on using $l = v_F \tau_q$, becomes

$$\Gamma = E_F, \quad (7)$$

where $E_F = \hbar^2 k_F^2 / 2m = (\hbar^2 / 2m)(4\pi n g_s g_v)$. We will use this modified Ioffe-Regel criterion in some of our theoretical analyses since this condition implies a non-universal critical resistivity ρ_c at the 2D MIT crossover even for the same values of g_s and g_v . We emphasize, however, that most of our results are derived based on the standard Ioffe-Regel criterion where l is taken as the transport mean free path. We mention that the condition defined by Eq. (7), which arises from assuming $k_F v_F \tau_q = 1$, is meaningful since extended metallic states described by momentum eigenstates cannot exist when the level broadening becomes equal to the Fermi energy since the momentum is then no longer a good quantum number. In ordinary metals, one always has $\tau_q = \tau_t$ and hence this issue becomes irrelevant.

We note, however, that the calculation of the crossover critical density n_c itself, either using the transport mean free path or the quantum mean free path, would give similar qualitative (but different quantitative) results. Since the precise sample disorder is never quantitatively known (and since we use approximations in treating disorder scattering effects), our goal in this work is a qualitative (and not quantitative) evaluation of the dependence of n_c on various physical variables such as disorder (i.e., n_i and d), mobility (at high density), temperature, magnetic field, and materials parameters (e.g., g_v, g_s).

We note that in most systems where the Ioffe-Regel criterion has been applied and discussed so far in the literature (see Graham *et al.*²³ and references therein) there is virtually no difference between the transport relaxation time τ_t and the quantum scattering time τ_q since the effective disorder potential is short-ranged. In high-mobility modulation-doped 2D systems, however, the charged dopants are placed far from the plane of the 2D layer where the carriers (either electrons or holes in n- or p-modulation doped GaAs or Si-Ge quantum wells and heterostructures) are located, leading to an essentially unscreened very long-range disorder potential in the 2D system. In such modulation-doped high-mobility 2D systems, it is possible for $\tau_t \gg \tau_q$ since most of the disorder scattering would be forward scattering, suppressing τ_q without affecting τ_t .²⁴ In such a situation, where forward scattering by remote dopants ($k_F d \gg 1$) dominates transport, it is possible for ρ_c given by Eq. (7) to be smaller than the ρ_c defined by Eq. (5). Consequently,

the crossover critical density n_c will then be higher as given by Eq. (7) with $\Gamma = \hbar/2\tau_q$ compared with that given by Eq. (1) with $l = v_F\tau_t$ defined by the transport mean free path. For Si-MOSFETs, most of the disorder is of short-ranged nature (either screened charged impurities near the interface or surface roughness scattering), and therefore, $\tau_t \approx \tau_q$, so that Eqs. (1) and (7) should give similar (but not identical) estimates for n_c and ρ_c with

$$\begin{aligned} n_c \text{ [obtained by Eq. (7)]} &\geq n_c \text{ [obtained by Eq. (1)]} \\ \rho_c \text{ [from Eq. (7)]} &\leq \rho_c \text{ [from Eq. (5)].} \end{aligned} \quad (8)$$

The inequalities given in Eq. (8) above are general applying to all 2D and 3D systems, and follow simply from the fact that $\tau_q \lesssim \tau_t$ always.

A. Theory

1. Disorder dependence

Starting with Eq. (1) and writing $l = v_F\tau$ where τ is an impurity-induced scattering time (either τ_t or τ_q), we can derive the following scaling relation

$$n_c \sim n_i^\gamma \quad (9)$$

where

$$\gamma = (1 + \delta)^{-1} \quad (10)$$

and the exponent ‘ δ ’ defines the density dependence of τ

$$\tau \sim n^\delta. \quad (11)$$

In deriving Eq. (9), we assume that all parameters, other than n_i , are fixed and disorder is entirely parameterized by the 2D impurity density n_i . There is an implicit dependence of n_c on the background dielectric constant κ and on the impurity location parameter d not explicitly shown in Eqs. (9) – (11). We assume (at this stage) that the d -parameter (and the dielectric constant κ) characterizing the samples is approximately a constant so that the disorder strength can be characterized by the single parameter 2D impurity density n_i in Eq. (9).

The sample mobility itself is, by definition, inversely proportion to n_i

$$\mu \sim n_i^{-1}, \quad (12)$$

enabling us to eliminate n_i in Eq. (9) in favor of some ‘‘maximum mobility’’ μ_m defined at a high fiduciary carrier density $n_m \gg n_c$. Eliminating n_i in favor of μ_m^{-1} we get

$$n_c \sim \mu_m^{-\gamma}. \quad (13)$$

This gives us a scaling relationship connecting the crossover density n_c to the sample quality as characterized by the typical ‘‘maximum mobility’’ μ_m defined at

some high carrier density $n_m \gg n_c$ deep in the metallic phase.

A detailed theory has recently been developed by us²⁵ for the density scaling of 2D metallic conductivity (and mobility), where we find that the exponent δ (with $\mu \sim n^\delta$) given by

$$\delta \approx 0.7 \text{ (n - GaAs); } 0.5 \text{ (p - GaAs); } 0.3 \text{ (n - Si),} \quad (14)$$

restricting to the $n \gg n_c$ situation. This then implies

$$\gamma = 1/1.7 - 1/1.3 \approx 0.59 - 0.77, \quad (15)$$

with

$$\gamma \approx 0.59 \text{ (n - GaAs), } 0.67 \text{ (p - GaAs); } 0.77 \text{ (n - Si).} \quad (16)$$

We emphasize that Eqs. (14) – (16) are very approximate and are derived assuming that the 2D impurity density n_i is the only variable determining the disorder, and therefore the quantitative applicability of the numerical values of the exponent γ (defining $n_c \sim \mu_m^{-\gamma}$) is very approximate. We note that for purely short-range δ -function scatterers, we get $\delta = 0$ and $\gamma = 1$, i.e., $n_c \sim n_i$ for purely zero-range disorder.

It is, therefore, important to emphasize that such a scaling relationship, $n_c \sim \mu_m^{-\gamma}$, with $\gamma \approx 0.67$ approximately (but with some fluctuations in the distribution of γ values around $\gamma \sim 0.67$) was noted empirically by Sarachik²⁶ more than ten years ago based on a careful numerical analysis of the existing 2D MIT experimental data. Thus, our Ioffe-Regel criterion based theoretical analysis of the dependence of the crossover critical density n_c on the typical sample mobility μ_m is consistent with the 2D MIT experimental data²⁶. This agreement between the experimental mobility dependence of n_c and our Ioffe-Regel criterion based results is one of the main *a posteriori* justifications for our theory.

Similar theoretical considerations can also be applied to the case where τ is interpreted to be the quantum scattering time τ_q [rather than the transport scattering time τ_t as in the analysis of Eqs. (9) – (16) above]. For this situation the Ioffe-Regel criterion is better written as $\Gamma = E_F$ [see Eq. (7)], and it is straightforward to show that we get the following results for n_c (where q_{TF} is the 2D Thomas-Fermi screening wave vector¹)

$$n_c = n_i q_{TF}^2 \int_0^1 \frac{dx}{\sqrt{1-x^2}} \frac{e^{-4k_F dx}}{(x + q_{TF})^2}, \quad (17)$$

which leads immediately to

$$n_c = \frac{1}{4\sqrt{2\pi}} \left(\frac{n_i}{d} \right)^{2/3} \text{ for } k_F d \gg 1, \quad (18)$$

and

$$n_c = \frac{\pi n_i}{2} \text{ for } k_F d \ll 1. \quad (19)$$

Assuming the impurity separation parameter ‘ d ’ to be fixed and the impurity density n_i to be the sole determinant of the system mobility, we can adapt Eqs. (17)

– (19) to provide a dependence of the critical density n_c on some fiduciary maximum mobility μ_m (defined as the sample mobility at some high characteristic density)

$$n_c \sim \mu_m^{-0.67} \text{ for } k_F d \gg 1, \quad (20)$$

and

$$n_c \sim \mu_m^{-1} \text{ for } k_F d \ll 1. \quad (21)$$

This immediately leads to the same conclusion we already discussed above [see the discussion above following Eq. (16)] that the dependence of n_c on the sample quality follows an approximate power law $n_c \sim \mu_m^{-\gamma}$ where $\gamma \approx 0.5 - 0.8$, as has been already pointed by Sarachik based on an empirical analyses of the experimental data²⁶. Thus, both the original Ioffe-Regel criterion $k_F l = 1$ and our modified Ioffe-Regel criterion $E_F = \Gamma$ give the same theoretical dependence of n_c on the sample mobility, which is in agreement with the existing experimental data on 2D MIT. We note that a pure short-range disorder model on the other hand gives the exponent $\gamma = 1$ disagreeing with the empirical data on 2D MIT.

2. Temperature dependence

The Ioffe-Regel criterion strictly applies at $T = 0$, but can be generalized to finite temperatures by considering the temperature dependence of the mean free path ‘ l ’ on the metallic side. This is, of course, relevant for the 2D MIT problem since its hallmark (and the *raison d’être* for its huge impact in contrast to the corresponding MIT phenomenon in 2D semiconductor systems in the 1970 – 90 era) is the strong temperature dependence of the 2D metallic conductivity for $n \gtrsim n_c$. The strong temperature dependence of the 2D metallic conductivity for $n \gtrsim n_c$ immediately leads to a strong temperature dependence of the mean free path $l(T)$, which should affect the critical density $n_c(T)$ derived on the basis of the Ioffe-Regel criterion $k_F l = 1$. Since the 2D metallic conductivity decreases with increasing temperature for $n \gtrsim n_c$, the corresponding $l(T)$ also decreases with increasing temperature whereas the Fermi wave vector $k_F \propto \sqrt{n}$ is, by definition, temperature-independent. This implies that $n_c(T)$, defined by the Ioffe-Regel criterion, increases with increasing temperature at the lowest temperatures, where strong metallicity is observed in high-quality 2D systems. The situation is, however, complicated by the fact^{27,28} that the 2D conductivity is non-monotonic as a function of temperature, and eventually decreases with increasing temperature for $T \gtrsim T_F$ which is reached at pretty low temperatures if $T_c = T_F(n_c)$ is low. Thus, $n_c(T)$ could manifest non-monotonic behavior as a function of temperature for a given sample with $n_c(T)$ increasing with T at the lowest temperatures, and then decreasing with T at higher temperatures. Using the Ioffe-Regel criterion and the Boltzmann transport

theory at finite temperatures^{27,28}, we get for $T \ll T_c$

$$n_c(T) \approx n_c \left[1 + \left(\frac{x_0}{1+x_0} \right) \frac{T}{T_c} \right], \quad (22)$$

and for $T \gtrsim T_c$

$$n_c(T) \sim \frac{T_c}{T}, \quad (23)$$

where $n_c = n_c(T = 0)$; $T_c = T_F(n = n_c)$, and $x_0 = q_{TF}/2k_{Fc}$ where $k_{Fc} = k_F(n = n_c)$. (We note that the screening wave vector q_{TF} is a constant independent of carrier density in 2D because of the constant 2D density of states.) From Eqs. (22) and (23), we conclude that $n_c(T)$ would in principle manifest non-universal behavior, but at sufficiently high temperatures, $n_c(T)$ will decrease with increasing temperature approximately linearly, *i.e.*, $n_c(T > T_c) \sim 1/T$. This $1/T$ decrease in $n_c(T)$ has been experimentally observed^{17,18,29}, however, the predicted increase of $n_c(T)$ with T at lower temperatures has not yet been reported in Si MOSFETs (although it has been seen in 2D p-GaAs holes¹⁸, perhaps because the lowest temperatures are not reached yet in the experiments to see this decrease or because of complications arising from weak localization corrections not included in our theory, which would dominate the asymptotic low-temperature transport).

3. Magnetic field dependence

One of the most important experimental discoveries³⁰ in the 2D MIT phenomena is the observation of a strong enhancement of n_c by the application of an applied parallel (to the 2D layer) magnetic field, which is equivalent to the suppression of the 2D effective metallic phase by the applied parallel field. In addition to the enhancement of n_c compared with its zero-field value, an applied parallel magnetic field also leads to a suppression of the metallic temperature dependence which becomes weaker as the applied field is made stronger. While this latter effect of the magnetic field induced weakening of the metallic temperature dependence has been extensively studied theoretically³¹, there has been no theoretical analysis in the literature of the magnetic field induced enhancement of n_c itself.

The Ioffe-Regel criterion provides a natural explanation for the field induced enhancement of n_c as arising from the suppression of the metallic mean free path ‘ l ’ (or the enhancement of the quantum level broadening Γ) due to the enhancement of the effective disorder in the metallic phase as the effective carrier screening is reduced by the application of the applied parallel magnetic field B . Screening is suppressed at finite B since the system gets spin polarized by the B -induced Zeeman splitting so that the effective Thomas-Fermi screening wave vector q_{TF} defined by

$$q_{TF} = \frac{g_s g_v m e^2}{\kappa \hbar^2}, \quad (24)$$

decreases as the spin degeneracy changes from $g_s = 2$ for $B = 0$ to $g_s = 1$ for $B = B_s$ where B_s is the density dependent field strength that completely spin-polarizes the 2D system, i.e., B_s is defined by

$$2g\mu_B B_s = E_F, \quad (25)$$

where g is the Landé g -factor for the specific semiconductor, μ_B is the Bohr magneton, and E_F is the Fermi energy at $B = 0$. For $B = B_s$, the 2D system is completely spin-polarized at the Fermi level with $g_s = 1$. We note, however, that $k_F = (4\pi n/g_s g_v)^{1/2}$ itself is now B -dependent in the presence of spin-polarization, and becomes $\sqrt{2}$ times larger at $B = B_s$ compared with its value at $B = 0$ since g_s decreases from 2 to 1. Thus, if the mean free path l remains unaffected by the applied field B , then the effect of spin-polarization-induced enhancement of k_F itself would lead to a decrease of n_c in finite B in apparent disagreement with experimental observations. Thus, spin-polarization-induced (or equivalently B -induced) suppression of screening (and the consequent enhancement of Coulomb disorder) is essential in understanding the enhancement of n_c in the presence of finite applied parallel field. If the effective disorder underlying the 2D MIT phenomenon is purely short-ranged δ -function white-noise disorder, where carrier screening should play no key role, then the application of the parallel magnetic field would decrease n_c , effectively enhancing the metallic phase rather than suppressing it as observed experimentally. This latter effect (but not the former), i.e., the effect of the enhancement of k_F by spin-polarization (but not the effect of suppressed screening), is already implicit in Eq. (9) which implies a decreasing n_c with decreasing g_s (i.e., with increasing applied field). We mention that for very large n_c , so that $q_{TF}/2k_F$ is very small and screening is unimportant, we do predict that an applied parallel field will either have almost no effect on n_c because spin-polarization effects are negligible due to the very small spin-polarization induced by an applied field at very large density (or will decrease it because of the increasing k_F with increasing spin-polarization). One reason that the applied field effect on 2D MIT was not discovered until 2000 is indeed the fact that n_c was simply too large in the older (and dirtier) 2D samples for the field-induced screening suppression to play any role.

To include the effect of suppressed screening in the presence of finite spin-polarization (i.e., $g_s < 2$), we must take into account the variation of q_{TF} with g_s as shown in Eq. (24). We can obtain an analytical formula by noting that the screened Coulomb disorder $u(q)$ behaves in the following manner

$$u(q) = \frac{v(q)}{\epsilon(q)} = \frac{2\pi e^2}{\kappa(q + q_{TF})}, \quad (26)$$

where $v(q) = 2\pi e^2/\kappa q$ is the unscreened 2D Coulomb interaction and $\epsilon(q) = 1 + q_{TF}/q$ is the 2D carrier dielectric screening function. In the strong screening limit

($q_{TF} \gg k_F$), we can write $u(q) \sim q_{TF}^{-1} \sim g_s^{-1}$, and this limit enables an analytical calculation by noting that $l^{-1} \propto n_i u^2 \propto n_i/g_s^2$, which allows us to replace n_i in Eq. (9) by n_i/g_s^2 , producing the following equation for $n_c(B)$ taking into account dual effects of the enhancement (suppression) of both k_F (q_{TF}) by the applied field compared with their $B = 0$ values

$$n_c(B) \sim \left(\frac{n_i}{g_s}\right)^\gamma, \quad (27)$$

which is valid in the strong screening ($q_{TF} \gg k_F$) limit. In the weak screening limit, the spin-polarization dependence in the screening may be ignored and we get

$$n_c(B) \sim (g_s n_i)^\gamma. \quad (28)$$

To obtain the explicit B -dependence of $n_c(B)$ we need to express the spin-degeneracy factor g_s as a function of the magnetic field B , which then leads to

$$n_c(B) \sim \left(1 + \frac{B}{2B_s}\right)^\gamma, \quad (29)$$

and

$$n_c(B) \sim \left(1 - \frac{B}{2B_s}\right)^\gamma, \quad (30)$$

respectively for Eqs. (27) and (28). Since the 2D MIT phenomenon mostly occurs in the strong-screening ($q_{TF} \gg k_F$) regime, Eq. (29) applies to most situations indicating an increase in the critical density with increasing applied field. At high carrier densities where $2k_F \gg q_{TF}$ or in a situation where short-range scattering dominates transport so that screening is not relevant, Eq. (30) should apply, and thus for highly disordered samples with large n_c (so that $q_{TF} \ll 2k_F$), it is conceivable that an applied field may slightly decrease n_c .

Before concluding this section we mention that all our considerations above for the effect of spin polarization g_s (as modulated by the parallel field B) apply equally well to the valley degeneracy g_v since the combination $g_s g_v$ appears in all physical quantities. In particular, if g_v could be modified somehow by an external valley-symmetry-breaking field A (for example, an applied strain), then Eqs. (29) and (30) will apply to describe the valley degeneracy dependence of the critical density with the A -field replacing the B -field. In both cases, the lifting of the spin (or valley) degeneracy by an external field would typically lead to an increasing critical density with increasing field since most 2D MIT phenomena happen in the $q_{TF} \gtrsim k_F$ strong screening regime [as characterized by Eq. (29)]. Indeed, such a symmetrical situation of increasing n_c with increasing external symmetry breaking field for either spin or valley degeneracy has been experimentally observed by Shayegan and his collaborators in the multivalley AIAs 2D systems³². Our qualitative findings in this section are in excellent agreement with these experimental results³² showing an

equivalence of increasing n_c with the decrease of g_s or g_v . In particular, a given sample with a fixed carrier density (n) is most likely to be in the insulating phase [i.e., $n < n_c(g_s, g_v)$] when the 2D system is maximally polarized to have the minimum possible values of g_s and g_v as precisely observed by Shayegan and his collaborators³².

4. Materials dependence

To consider how n_c depends on the materials parameters (e.g., m , κ , g_s , g_v) of the 2D system we imagine a situation with fixed bare disorder (i.e., fixed n_i and d) while varying only the materials parameters to see how the Ioffe-Regel criterion $k_F l = 1$ is affected.

Expressing the mean free path $l = v_F \tau$ in terms of the relaxation time τ , and then using the Boltzmann equation to obtain τ assuming scattering from random screened charged impurities we get the following integral equation for n_c from the Ioffe-Regel condition (at $T = 0$) $k_F l = 1$

$$\frac{1}{\tau} = \frac{\hbar k_F^2}{m} = \frac{n_i m}{\pi \hbar^3 k_F^2} \left(\frac{2\pi e^2}{\kappa} \right)^2 \int_0^1 \frac{dy}{\sqrt{1-y^2}} \frac{y^2 e^{-2y d_0}}{(y+x)^2}, \quad (31)$$

where $x = q_{TF}/2k_F$ and $d_0 = 2k_F d$. All other quantities in Eq. (31) are defined with $k_F = (4\pi n/g_s g_v)^{1/2}$ and $q_{TF} = g_s g_c m e^2 / \kappa \hbar^2$. We can rewrite the integral equation defined by Eq. (31) as

$$\pi \hbar^4 k_F^4 = n_i m^2 \left(\frac{2\pi e^2}{\kappa} \right)^2 \int_0^1 \frac{dy}{\sqrt{1-y^2}} \frac{y^2 e^{-2d_0 y}}{(y+x)^2}. \quad (32)$$

We note that Eq. (32) is a nontrivial integral equation for n_c since the density n enters the equation in three distinct places: $k_F \propto \sqrt{n}$, $d_0 = 2k_F d$, and $x = q_{TF}/2k_F \propto n^{-1/2}$. Before discussing the materials dependence of n_c implied by Eq. (32), we note that the above relationship [i.e., Eq. (32)] has been derived by assuming ‘ l ’ to be the transport mean free path, i.e., $\tau = \tau_t$. If, instead of τ_t we use the quantum relaxation time $\tau = \tau_q$, the only difference is that the vertex correction term disappears from the integral on the right hand side, leading to the following integral equation for $n = n_c$ using the $\Gamma = E_F$ Ioffe-Regel criterion (i.e. $\tau = \tau_q$ in $k_F l = k_F v_F \tau = 1$)

$$\pi \hbar^4 k_F^4 = n_i m^2 \left(\frac{2\pi e^2}{\kappa} \right)^2 \int_0^1 \frac{dy}{\sqrt{1-y^2}} \frac{e^{-2d_0 y}}{(y+x)^2}, \quad (33)$$

with the only difference between Eqs. (32) and (33) being the additional factor of y^2 inside the integral on the right hand side of Eq. (32) – this y^2 factor arises from the well-known ‘ $1 - \cos \theta$ ’ vertex correction term in the Kubo formula for the current-current correlation function in the conductivity.

In Eqs. (32) and (33), materials parameters m , g_s , g_v , κ enter through $k_F = (4\pi n/g_s g_v)^{1/2}$, $d_0 = 2k_F d$,

$x = q_{TF}/2k_F = (g_s g_v)^{3/2} m e^2 / (4\kappa \hbar^2 \sqrt{\pi n})$, and the factor $2\pi e^2/\kappa$ as well as m on the right hand side. It is obvious that no definitive and unique dependence of $n_c = n_c(g_v, g_s, m, \kappa)$ on the materials parameters can be analytically discerned from Eqs. (32) and (33) because of the complex functional relationship defined by Eqs. (32) and (33) of the form $n^2 = n_i A(g_v, g_s, m, \kappa) \int_0^1 dy f(y; n, d, g_v, g_s, m, \kappa)$ where both A and f are functions of the materials parameters g_v , g_s , m , and κ . The only relatively simple dependence implied by the integral equations (32) and (33) is the dependence on the impurity density n_i , which has already been discussed in subsection II A 1 above in details. We mention here that using the Ioffe-Regel criterion the $k_F d \gg 1$ and $k_F d \ll 1$ limits of Eqs. (32) and (33) lead to $n_c \sim (n_i/d)^{2/3}$ and $n_c \sim n_i d^0$, respectively.

To discuss the materials dependence of n_c analytically, we start by assuming that the strong screening ($q_{TF} \gg 2k_F$) condition applies to the 2D system, which is likely (since n_c is relatively low for the 2D MIT phenomenon to manifest itself), but not guaranteed. An additional constraint is necessary on the dimensionless variable $d_0 = 2k_F d$, which we also assume to be small (which certainly applies to Si-MOSFETs, but may not always apply to the modulation-doped GaAs structures even at low values of n_c). With these two constraints (i.e., $q_{TF} \gg 2k_F$ and $2k_F d \ll 1$), the Ioffe-Regel integral equation can be analytically studied to provide the following approximate asymptotic dependence of n_c on materials parameters

$$n_c \sim (g_s g_v)^{-2/3}; \quad n_c \sim \kappa^{2/3}; \quad n_c \sim m^0. \quad (34)$$

It is interesting and important to note that in the strong-screening ($q_{TF} \gg 2k_F$) limit, there is no dependence of the critical density n_c on the effective mass of the system since the effective mass appearing in q_{TF} (i.e., screening) exactly cancels out the inverse effective mass appearing in the Fermi velocity in this artificial limit $q_{TF} \gg 2k_F$. The spin- and valley-degeneracy dependence shown in Eq. (34) is the same as what we obtained in subsection II A 3 above, and indicates that in general insulating (metallic) phase is preferred by lower (higher) values of g_s or g_v . We note, however, that the strong-screening situation itself, $q_{TF} \gg 2k_F$, depends crucially on the effective mass since $q_{TF} \sim m$, and thus the strong screening condition is difficult to achieve in 2D systems with small effective mass.

5. Comparison with percolation transition

Ioffe-Regel criterion provides one possibility for conductor-to-insulator crossover in 2D semiconductor systems. Another possibility, which has been studied rather extensively in the 2D MIT literature^{17,18,29,33-36}, is a classical percolation transition at $n = n_c$ arising from the 2D Fermi level moving through the potential fluctuations (“mountains and lakes” landscape) associated with the long-range Coulomb disorder in the 2D system.

Simple theoretical considerations³⁵ and direct numerical simulations³⁶ indicate that a percolation conductor-to-insulator transition may occur at a critical carrier density given by

$$n_c \approx \frac{1}{4\pi} \frac{\sqrt{n_i}}{d} \approx 0.1 \frac{\sqrt{n_i}}{d}, \quad (35)$$

where the long-range-Coulomb disorder is created in the 2D layer by random charged impurities of 2D density n_i located a distance ‘ d ’ from the 2D layer (i.e., exactly the same model for disorder we have used in this work for applying the Ioffe-Regel criterion $k_F l = 1$). Since the percolation transition in the context of 2D MIT has already been extensively studied in the literature, we do not provide any details in the current work on the percolation transition and accept Eq. (35) for the crossover density as a given. Our goal in the current work is to compare the percolation transition with the Ioffe-Regel transition in the context of the 2D MIT phenomena. It is, however, important here to point out that the percolation transition is manifestly a classical phenomenon with the MIT being driven by the chemical potential or the Fermi level (which is proportional to the carrier density in 2D) crossing through the percolation point in the potential fluctuation driven inhomogeneous 2D “mountains and lakes” landscape with the high-density ($n \gg n_c$) metallic phase being essentially the homogeneous (and well-screened) “all-lakes” conducting situation whereas the low-density ($n \ll n_c$) insulating phase being the highly inhomogeneous (and unscreened) “all-mountains” situation. By contrast, the Ioffe-Regel criterion defines a completely quantum condition for the localization crossover. In some loose sense, the two criteria (percolation and Ioffe-Regel) are complementary and describe the 2D MIT as a high-temperature classical and a low-temperature quantum crossover phenomenon, respectively.

We note that for fixed ‘ d ’, the percolation criterion implies $n_c \sim \sqrt{\mu_m}$, i.e., the exponent [see. Eqs. (9) and (13)] $\gamma = 1/2$ in the percolation picture whereas $\gamma \approx 0.6 - 0.8$ in the Ioffe-Regel theory as discussed already in great details above. If we assume n_i to be fixed and ‘ d ’ to be the relevant variable characterizing impurity disorder, then the percolation theory gives the simple dependence $n_c \sim d^{-1}$, which can be converted to the following dependence on the high-density mobility μ_m assuming that $k_F d \gg 1$ condition applies

$$n_c \sim d^{-1} \sim \mu_m^{-1/3}, \quad (36)$$

where we have used the fact that 2D mobility $\mu \sim d^3$ for $k_F d \gg 1$ (and fixed n_i). Thus percolation theory gives the following exponent γ (where $n_c \sim \mu_m^\gamma$) for the critical density, assuming d to be fixed,

$$\gamma = 1/2, \quad (37)$$

and, assuming n_i to be fixed,

$$\gamma = 1/3. \quad (38)$$

In addition, the percolation critical density, being dependent only on n_i and d (i.e., just the bare disorder), is independent of materials parameters g_v , g_s , m , and κ in contrast to the critical density n_c based on the Ioffe-Regel criterion. We mention the corresponding Ioffe-Regel exponents for Eqs. (37) and (38) are $\gamma = 2/3$ (fixed d) and $2/9$ (fixed n_i) for $k_F d \gg 1$. The differences in the exponent γ between the two theories are significant ($\gamma = 1/2$ and $1/3$ versus $\gamma = 2/3$ and $2/9$, respectively), but not very large.

One particular aspect of percolation induced 2D MIT not discussed above is worth mentioning here (and we will present numerical results on this aspect later in this paper). The critical density defined by percolation theory is completely independent of any transport considerations and thus the constraint on the critical resistivity $\rho_c \lesssim (2/g_s g_v)(h/e^2)$ defined by Eqs. (5) and (8) does not apply to the percolation critical resistivity. In principle, therefore, ρ_c for the 2D MIT percolation crossover could be any value much larger or smaller than the quantum resistance value of h/e^2 whereas, by contrast, the Ioffe-Regel condition implies a critical resistance of $O(h/e^2)$. In practice, however, we find numerically (as shown in the next section) that the calculated $\rho_c = \rho(n_c)$ at the 2D MIT percolation transition turns out to be $\sim h/e^2$ for most, if not all, 2D MIT experimental parameters in realistic 2D systems. The possibility, however, remains that ρ_c could be very different from h/e^2 in a percolation 2D MIT crossover since the percolation transition is simply a classical transition between immobile and mobile states depending on the value of the chemical potential (i.e., the Fermi level) with respect to the disorder potential in an inhomogeneous potential fluctuation landscape where localization or quantum interference plays no role.

While the fact that the percolation critical resistivity $\rho_c = \rho(n = n_c)$ is, in principle, arbitrary (and can be larger or smaller than h/e^2 with no theoretical constraint) may appear to be an attractive quantitative feature of the percolation theory in describing 2D MIT, there are other aspects of the percolation transition which are in manifest disagreement with the experimental phenomenology for 2D MIT even on a qualitative level. For example, the percolation theory predicts an $n_c = n_c(n_i, d)$ which is completely independent of materials parameters (i.e., m , κ , etc.) and of the valley and/or spin degeneracy. This is in disagreement with experimental findings for 2D MIT where, for example, applying an external in-plane magnetic field to spin-polarize the 2D system leads to an increasing n_c which cannot easily be described by the percolation theory. The classical percolation theory would predict no dependence of n_c on an applied magnetic field.

B. Numerical Results

We now present detailed numerical results for our calculated critical crossover density n_c as a function of var-

ious physical parameters using the Ioffe-Regel criterion. These results are obtained by directly numerically solving the integral equations defined by Eq. (32) or (33), which correspond respectively to using $l_t = v_F \tau_t$ or $l_q = v_F \tau_q$ in the Ioffe-Regel criterion $k_F l = 1$. Both equations give similar qualitative results, and our goal in this work is an investigation of the qualitative dependence of n_c on disorder, temperature, applied in-plane magnetic field, and system parameters, and we do not therefore distinguish between these two closely related versions (i.e., l_t or l_q) of the Ioffe-Regel criterion. We also provide a comparison between n_c^{IR} and n_c^{per} as obtained respectively by the Ioffe-Regel criterion and percolation transition in same situations. We believe that a direct comparison between n_c^{IR} and n_c^{per} as a function of disorder could shed considerable light on the nature of the 2D MIT, in particular, distinguishing between quantum localization and classical percolation on a qualitative level.

1. Pure 2D case

In Fig. 1, we show our numerically calculated critical density n_c for both the Ioffe-Regel and the percolation theory as a function of n_i (with d fixed) and d (with n_i fixed). All numerical results presented in this subsection assume the 2D carriers to be confined in an ideal strict 2D layer of zero thickness. For the percolation theory, of course, $n_c = 0.1\sqrt{n_i}/d$ is trivial to plot, and we provide these results only for the sake of comparison with the nontrivial Ioffe-Regel results for n_c , which we obtain by numerically solving the integral equation defined by Eq. (33), which uses $\tau = \tau_q$ (i.e., $\Gamma = E_F$ Ioffe-Regel condition). We show results for the three most commonly studied 2D systems: n-GaAs, p-GaAs, and n-Si(100)-MOSFET (using the appropriate corresponding values of m , κ , g_v , etc. in solving the integral equation for n_c).

Several general comments can be made about the results shown in Fig. 1: (i) The analytically derived scaling behavior derived earlier in this paper apply in their respective regimes of validity, but the dependence of n_c on both (n_i, d) characterizing disorder precludes any definitive dependence of n_c on the system mobility since $n_c(n_i, d)$ and $\mu_m(n_i, d)$ at some high density $n_m \gg n_c$ are two independent functions of n_i and d . (ii) In general, $n_c^{IR} > n_c^{per}$ for larger values of n_i and/or d . We see the clear trend in Fig. 1 that as n_i (d) increases for fixed d (n_i) respectively, n_c^{IR} lines cross above the n_c^{per} lines for all three 2D systems we study. For lower disorder (i.e., smaller n_i), which is of particular interest to 2D MIT phenomena, n_c^{IR} always is smaller than n_c^{per} . We expect the percolation theory to be of validity only for rather large values of d (since only then the Coulomb disorder is effectively unscreened and leads to long-range potential fluctuations in the 2D landscape), and again for ' d ' not too large, we always find $n_c^{IR} < n_c^{per}$. (iii) For similar disorder parameters (i.e., same values of n_i and d), our results in Fig. 1 indicate very similar (but not identical)

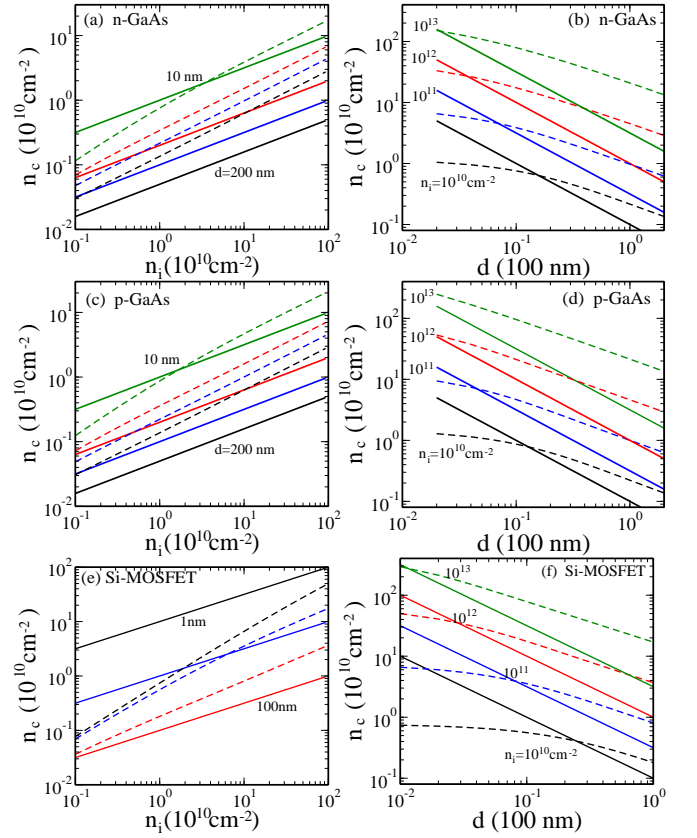


FIG. 1. The calculated critical density of n-GaAs (a) as a function of impurity density n_i for fixed impurity locations $d = 10, 50, 100, 200$ nm (from top to bottom) and (b) as a function of impurity location d for fixed impurity densities. Solid (dashed) lines represent the percolation critical density, n_c^{per} (Ioffe-Regel critical density, n_c^{IR}). (c) and (d) show the results for p-GaAs with the same impurity parameters of (a) and (b), respectively. (e) and (d) show n_c for Si-MOSFET. In (e) the impurity locations $d = 1, 10, 100$ nm (from top to bottom) are used.

values of n_c^{IR} for all three systems we study – of course $n_c^{per} = 0.1\sqrt{n_i}/d$ is, by definition, independent of the materials parameters. This finding of similar n_c^{IR} in all three systems, while being surprising at first sight, turns out to be consistent with experimental observations where the discrepancy in the reported n_c values among different systems (with $n_c^{Si} \sim 10^{11} \text{ cm}^{-2} > n_c^{p-GaAs} \sim 10^{10} \text{ cm}^{-2} > n_c^{n-GaAs} \sim 10^9 \text{ cm}^{-2}$) appears to arise almost entirely from the very different disorder parameters in these systems (with $\mu_m^{Si} \sim 5 \times 10^4 \text{ cm}^2/\text{Vs} < \mu_m^{p-GaAs} \sim 5 \times 10^5 \text{ cm}^2/\text{Vs} < \mu_m^{n-GaAs} \sim 5 \times 10^6 \text{ cm}^2/\text{Vs}$), where μ_m is the typical high-density mobility value, more or less explain the difference in their observed n_c values based on the approximate scaling law $n_c \sim \mu_m^{-\gamma}$. (iv) To the extent the numerical results in Fig. 1 allow us to discern any materials trend in the n_c^{IR} values, we find that for the same disorder strength (i.e., same values of n_i and d) Si-MOSFETs tend to have the lowest n_c^{IR} with n-GaAs and p-GaAs having almost the same calculated n_c , thus

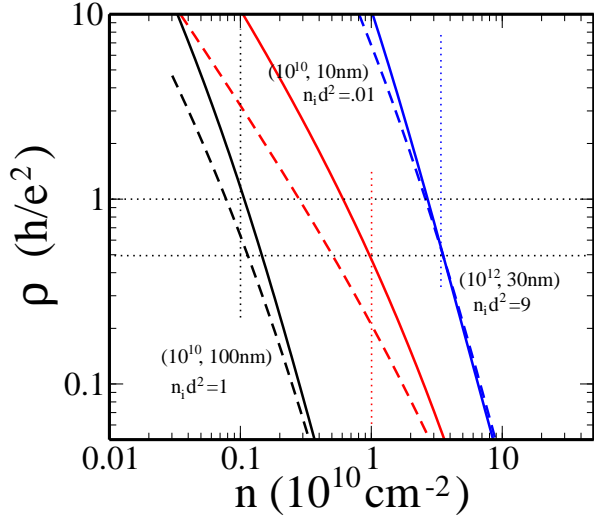


FIG. 2. The calculated resistivity ρ as a function of carrier density. The solid (dashed) lines show results for n-GaAs (Si-MOSFET). The sets of the remote impurity density n_i and the distance d are $(10^{10} \text{ cm}^{-12}, d = 100 \text{ nm})$ (i.e., $n_i d^2 = 1$); $(n_i = 10^{10} \text{ cm}^{-12}, d = 10 \text{ nm})$ (i.e., $n_i d^2 = 0.01$); $(n_i = 10^{12} \text{ cm}^{-12}, d = 30 \text{ nm})$ (i.e., $n_i d^2 = 9$) [from left to right]. The vertical dot lines indicate the percolation critical density for given impurity conditions (i.e., $n_c = 0.1\sqrt{n_i}/d$).

verifying the effective mass independence of n_c^{IR} we derived before. A clear prediction of this finding is that 2D n-GaAs and 2D p-GaAs will have very similar values of n_c provided they have similar disorder configurations.

To reinforce the point that the Ioffe-Regel criterion typically leads to n_c values which depend strongly on the disorder, but only weakly on the material, we show in Fig. 2 our calculated resistivity $\rho(n)$ as a function of 2D carrier density n for the n-Si-MOSFET and the n-GaAs system for exactly the same set of values of (n_i, d) with three different sets of disorder configurations (i.e., n_i and d values) shown in the plots. The $k_F l = 1$ Ioffe-Regel criterion translates into $\rho = h/e^2$, which gives similar n_c values for the three sets of disorder shown in Fig. 2. For the purpose of comparison we also shown $n_c^{per} = 0.1\sqrt{n_i}/d$, which again is reasonably close to the calculated n_c^{IR} value for each disorder configuration. At first sight, it appears that for the intermediate disorder strength (red curves with $n_i d^2 = 0.1$), the n_c^{IR} values for Si and n-GaAs are very different from each other, but this discrepancy is resolved once the valley degeneracy effect (i.e. $g_v = 2$ for Si) is taken into account so that the critical resistivity $\rho_c = h/2e^2$ for the Si system. It becomes clear that if we use $\rho_c^{Si} = 0.5h/e^2$ and $\rho_c^{GaAs} = h/e^2$, then indeed the resultant n_c values for the two systems are very close to each other, indicating the approximate materials universality of n_c among different 2D systems, with disorder being the primary determinant of n_c .

One unexpected aspect of the results shown in Fig. 2 is that the critical resistivity $\rho_c = \rho(n_c)$ for the percolation transition seems to be not very different from that (i.e.,

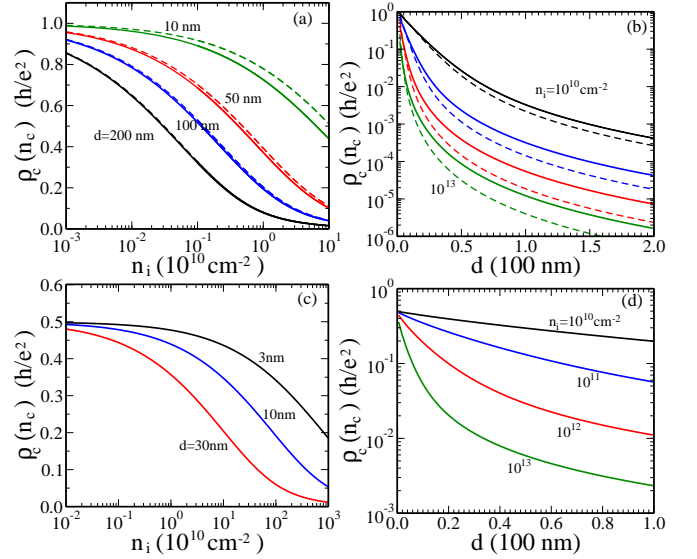


FIG. 3. The calculated resistivity ρ_c at Ioffe-Regel critical density, n_c^{IR} , (a) as a function of n_i for different $d = 10, 50, 100, 200 \text{ nm}$ and (b) ρ_c as a function d for different impurity densities $n_i = 10^{10}, 10^{11}, 10^{12}, 10^{13} \text{ cm}^{-2}$ (from top to bottom). The solid (dashed) lines are the results of n-GaAs (p-GaAs). (c) and (d) show the calculated resistivity ρ_c for a n-Si-MOSFET (c) as a function of n_i for different $d = 3, 10, 30 \text{ nm}$ and (d) as a function d for different impurity densities $n_i = 10^{10}, 10^{11}, 10^{12}, 10^{13} \text{ cm}^{-2}$.

$\rho_c \sim h/e^2$) implied by the Ioffe-Regel criterion, which is, of course, a direct manifestation of n_c^{per} and n_c^{IR} being not that different (typically $n_c^{per} \gtrsim n_c^{IR}$ in Figs. 1 and 2) from each other. We show in Figs. 3 – 6 our calculated ρ_c^{IR} and ρ_c^{per} defined by

$$\begin{aligned} \rho_c^{IR} &= \rho(n = n_c^{IR}), \\ \rho_c^{per} &= \rho(n = n_c^{per}). \end{aligned} \quad (39)$$

Although we expect $\rho_c^{IR} \lesssim h/e^2$, by definition, there is no reason for ρ_c^{per} to have anything to do with h/e^2 since it is a nonuniversal quantity not determined by quantum interference or quantum localization. Our results, however, indicate that in general $\rho_c^{per} \lesssim h/e^2$ as well!

In Fig. 3 we show our numerically calculated ρ_c^{IR} as a function of n_i and d for 2D n-GaAs, p-GaAs, and n-Si-MOS systems. We emphasize that $\rho_c^{IR} = 2h/(g_s g_v e^2)$ universally by definition if the quantity ‘ l ’ in the $k_F l = 1$ Ioffe-Regel criterion is interpreted as the transport mean free path [see Eq. (5)] of the 2D system. This means that $\rho_c^{IR} = h/e^2$ (GaAs); $h/2e^2$ (Si) for all n_i and d if we take ‘ l ’ to be the transport mean free path $l = l_t$ as in Eq. (32). All our numerical ρ_c^{IR} results therefore interpret $l = l_q$ as the quantum mean free path [using Eq. (33) without the conductivity vertex correction term] where $k_F l_q = 1$ becomes equivalent to $\Gamma = E_F$ strong localization condition. The most important qualitative conclusion based on the numerical results of Fig. 3 is that ρ_c^{IR} is large (small) for small (large) n_i and small (large) d . In Fig. 3

$\rho_c(n_i, d)$ falls off monotonically either as a function of increasing n_i or increasing d , which of course makes sense since small n_i and d implies very small n_c , and hence rather large ρ_c^{IR} (which is still bounded from above by h/e^2 since $\rho_c^{IR} \leq h/e^2$ by definition since $l_q \leq l_t$). The decrease of ρ_c^{IR} to incredibly small values as a function of increasing n_i or d may appear completely unphysical (perhaps even ridiculous) at first, but this is a direct manifestation of our model of disorder which is entirely characterized by a 2D impurity plane containing n_i random charged impurities per unit area separated by a distance ' d '. For large ' d ', this model fails completely since there would always be some unknown and unintentional background charged impurities which will cause the strong localization crossover at some higher value of ρ_c (i.e., lower value of n_c). In principle, however, the qualitative result emerging from Fig. 3 is that more disordered the system (i.e., larger the value of n_i), lower is the critical resistance ρ_c at the transition (and higher is the n_c). This is certainly qualitatively correct since older MOSFETs (before 1994 – 95 when the current era of 2D MIT physics commenced with the Kravchenko *et al.* work²²) typically had¹ very high values of n_c ($> 10^{12} \text{ cm}^{-2}$) with consequently rather low values of ρ_c ($\sim h/10e^2 \approx 2 \text{ k}\Omega$)¹. We also mention in this context the empirical finding of Sarachik²⁶ that $n_c \sim \mu_m^{-0.67}$ which implies very large n_c (and hence rather low ρ_c) for samples with very large values of n_i (i.e., low values of μ_m). Results with very large d -values in Fig. 3 are shown only for the sake of completeness since other unknown disorder with small ' d ' (not included in the model) will intervene making our large d results inapplicable to experimental systems. Our results, however, do indicate that extremely pure modulation doped 2D samples with large values of ' d ' should have relatively small values of ρ_c if all other disorder effects are absent. This theoretical prediction should be experimentally tested in the future.

In Fig. 4 we show the same results as in Fig. 3 except now for the percolation theory (i.e. ρ_c^{per} is shown as a function of n_i and d in Fig. 4 in contrast to Fig. 3 where ρ_c^{IR} is shown). It is clear that ρ_c^{per} (Fig. 4) behaves qualitatively very differently than ρ_c^{IR} (Fig. 3) with $\rho_c^{per} \sim h/e^2$ within a factor of 2 for most values of n_i and d . (We emphasize again that $\rho_c^{IR} = h/e^2$ within a factor of 2 also if the Ioffe-Regel criterion is taken to be $l = l_t$ in the $k_F l = 1$ condition.) The fact that the percolation transition which defines $n_c^{per} = 0.1\sqrt{n_i}/d$ with $\rho_c^{per} = \rho_c(n_c)$ as obtained from our standard Drude-Boltzmann semiclassical transport theory provides a very reasonable value of $\rho_c \sim h/e^2$ for a wide range of realistic disorder parameters is certainly somewhat of a surprise. We should mention that for unrealistically large n_i and/or unrealistically small d , ρ_c^{per} takes on unrealistic values, but for realistic physical combinations of (n_i, d) values operational in real 2D systems our theoretical ρ_c^{per} seems to agree well with the experimental results. We do not know at this stage whether this is simply a coincidence or indicates some deep truth about the importance

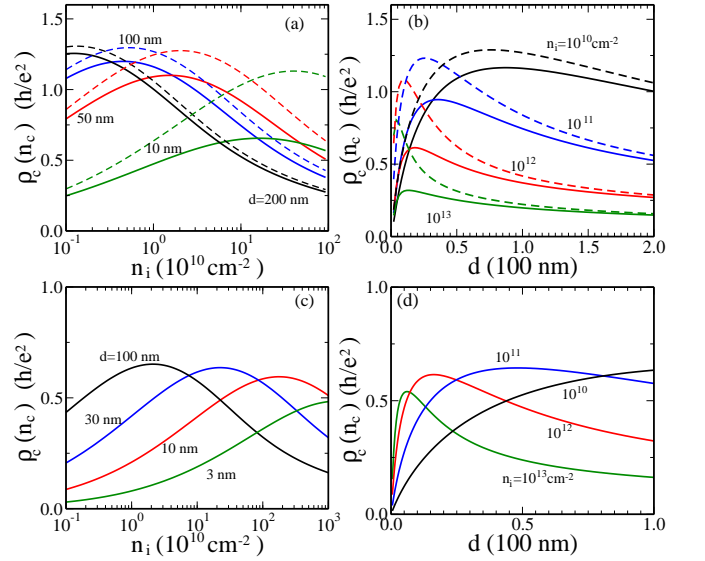


FIG. 4. The calculated resistivity ρ_c at percolation critical density, n_c^{per} , (a) as a function of n_i for different $d = 100, 50, 100, 200 \text{ nm}$ and (b) as a function of d for different impurity densities $n_i = 10^{10}, 10^{11}, 10^{12}, 10^{13} \text{ cm}^{-2}$. The solid (dashed) lines are the results of n-GaAs (p-GaAs). (c) and (d) show the calculated resistivity ρ_c for a n-Si-MOSFET (c) as a function of n_i for different $d = 3, 10, 30, 100 \text{ nm}$ and (d) as a function of d for different impurity densities $n_i = 10^{10}, 10^{11}, 10^{12}, 10^{13} \text{ cm}^{-2}$.

of percolation transport in the 2D MIT phenomena.

Results shown in Figs. 3 and 4 hint at the dimensionless parameter $n_i d^2$ being the important disorder parameter determining ρ_c^{IR} and ρ_c^{per} . This, in fact, follows from the definitions of these two critical resistivities. Using the Boltzmann transport theory for charged impurity scattering limited transport at $T = 0$,²⁵ we find

$$\rho_c = \frac{8h}{e^2} \frac{n_i}{n_c} x_c^2 \int_0^1 dy \frac{dy}{\sqrt{1-y^2}} \frac{y^2 e^{-2y d_c}}{(y+x_c)^2}, \quad (40)$$

where

$$k_c = k_F(n_c) = \left(\frac{4\pi n_c}{g_s g_v} \right)^{1/2}; \quad x_c = q_{TF}/2k_c; \quad d_c = 2k_c d. \quad (41)$$

Putting n_c^{per} or n_c^{IR} for n_c in Eq. (40) we obtain ρ_c^{per} and ρ_c^{IR} respectively. We note that the explicit dependence of $\rho_c \sim n_i$ in Eq. (40) is misleading since n_c itself has an n_i dependence also.

The integral on the right hand side of Eq. (40) can be analytically evaluated in various asymptotic limits for both ρ_c^{IR} and ρ_c^{per} , giving the following results (with $k_c \sim \sqrt{n_c}$): For $k_c d \gg 1$

$$\begin{aligned} \rho_c^{IR} &\propto (n_i d^2)^{-2/3}; \quad n_c \sim (n_i/d)^{2/3}, \\ \rho_c^{per} &\propto (n_i d^2)^{-1/4}; \quad n_c \propto \sqrt{n_i}/d. \end{aligned} \quad (42)$$

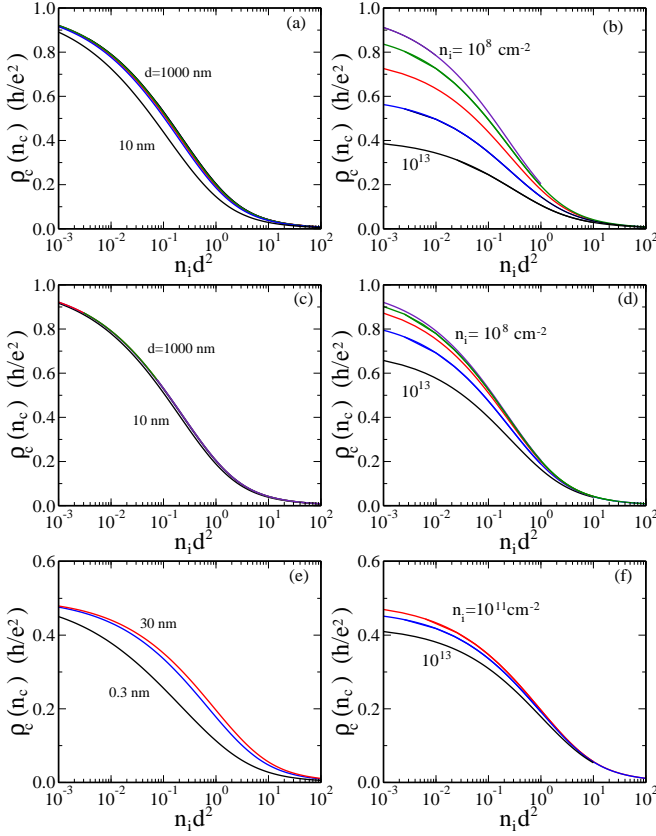


FIG. 5. (a) and (b) show the calculated resistivity at Ioffe-Regel critical density n_c^{IR} , ρ_c^{IR} , for n-GaAs as a function of $n_i d^2$ (a) varying n_i for various fixed $d = 10, 50, 100, 200, 1000$ nm (from bottom to top) and (b) varying d for various fixed $n_i = 10^8, 10^{10}, 10^{11}, 10^{12}, 10^{13}$ cm $^{-2}$ (from top to bottom), respectively. (c) and (d) show ρ_c^{IR} for p-GaAs with the same impurity parameters used in (a) and (b), respectively. (e) and (f) show ρ_c^{IR} as a function of $n_i d^2$ for Si-MOSFET (e) varying n_i for various fixed $d = 0.3, 3, 30$ nm (from bottom to top) and (f) varying d for various fixed $n_i = 10^{11}, 10^{12}, 10^{13}$ cm $^{-2}$ (from top to bottom), respectively.

For $k_c d \ll 1$

$$\begin{aligned} \rho_c^{IR} &\propto (n_i d^2)^{-3/2}; \quad n_c \sim n_i d^0, \\ \rho_c^{per} &\propto (n_i d^2)^{1/2}; \quad n_c \propto \sqrt{n_i}/d. \end{aligned} \quad (43)$$

This shows that $n_i d^2$ is an important dimensionless parameter determining the disorder scaling of the crossover resistivity ρ_c . We have explicitly checked numerically that these equations [Eqs. (42) and (43)] are in quantitative agreement of our numerical results.

We note that ρ_c and n_c have very different qualitative dependence on the disorder parameters n_i and d , and this might enable an experimental distinction between them possible if quantitative information about the underlying disorder becomes available. In Figs. 5 – 7 we show our numerically calculated ρ_c as a function of $n_i d^2$ to explicitly depict the dimensionless dependence of $\rho_c/(h/e^2)$ on the dimensionless disorder parameter $n_i d^2$.

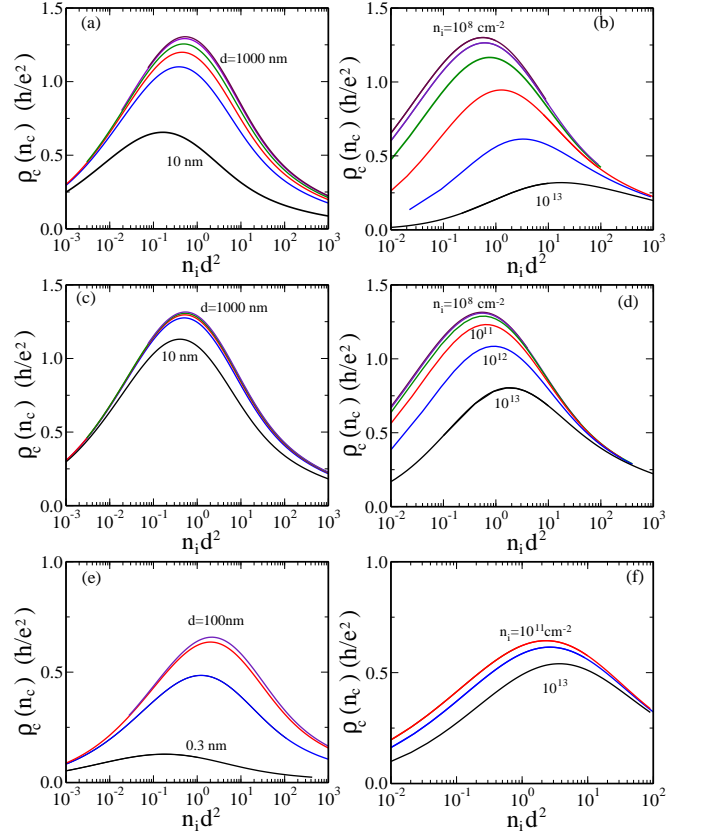


FIG. 6. (a) and (b) show the calculated resistivity at percolation critical density n_c^{per} , ρ_c^{per} , for n-GaAs as a function of $n_i d^2$ (a) varying n_i for various fixed $d = 10, 50, 100, 200, 1000$ nm (from bottom to top) and (b) varying d for various fixed $n_i = 10^8, 10^{10}, 10^{11}, 10^{12}, 10^{13}$ cm $^{-2}$ (from top to bottom), respectively. (c) and (d) show ρ_c^{per} for p-GaAs with the same impurity parameters used in (a) and (b), respectively. (e) and (f) show ρ_c^{per} as a function of $n_i d^2$ for Si-MOSFET (e) varying n_i for various fixed $d = 0.3, 3, 30, 100$ nm (from bottom to top) and (f) varying d for various fixed $n_i = 10^{11}, 10^{12}, 10^{13}$ cm $^{-2}$ (from top to bottom), respectively.

In Figs. 5 and 6 we show our calculated ρ_c^{IR} and ρ_c^{per} as a function of $n_i d^2$ for various fixed values of n_i and d (as shown in the figures) for 2D n-GaAs, p-GaAs, and n-Si-MOSFET systems. It is clear (which is also obvious from our analytical results) that the Ioffe-Regel and the percolation criteria provide very different qualitative dependence of ρ_c on disorder parameters. Finally, in Fig. 7 we show the calculated resistivity ρ at different values of $n \geq n_c^{per}$ in order to emphasize the scaling behavior.

2. Realistic 2D structures

All results shown in Figs. 1 – 7 are for strict zero-thickness 2D systems with the appropriate effective mass, lattice dielectric constant, and valley degeneracy ($g_v = 1, 2$ for GaAs, Si, respectively) defining each semiconductor material. Results given in Figs. 1 – 7 serve to provide

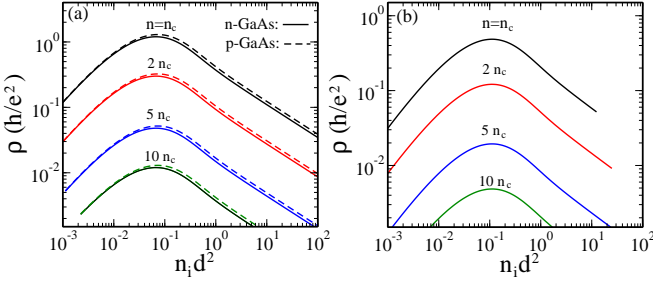


FIG. 7. The calculated resistivity ρ_c^{per} as a function of $n_i d^2$ (a) for n- and (solid lines) p-GaAs (dashed lines), and (b) for Si-MOSFET. In (a) and (b) $d = 100$ nm and $d = 3$ nm are used respectively. The percolation critical density $n_c = 0.1\sqrt{n_i}/d$ is calculated by changing n_i . The resistivity ρ is calculated at different values of $n \geq n_c^{per}$ in order to show the scaling behavior.

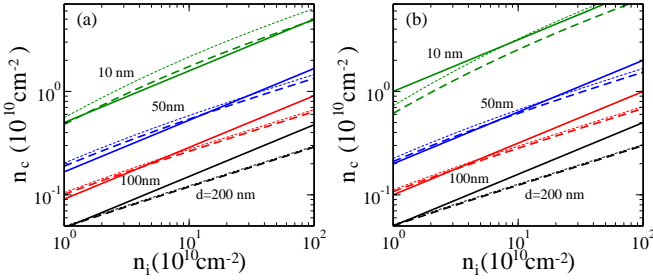


FIG. 8. (a) Calculated n_c^{IR} (dashed lines) and n_c^{per} (solid lines) as a function of impurity density for fixed several $d = 10, 50, 100, 200$ nm for GaAs quantum wells with a well width $a = 200$ Å. Thick (thin) dashed lines represent results for n-GaAs (p-GaAs). (b) The same results as (a) for zero quantum well thickness (i.e., $a = 0$).

the qualitative dependence of the critical density and resistivity on disorder parameters, but are not quantitatively realistic even if the disorder parameters (i.e., n_i and d) were precisely known. In particular, the finite quantum thickness of the realistic quasi-2D system softens the Coulomb disorder arising from the charged impurities since the 2D Coulomb interaction changes from $2\pi e^2/\kappa q$ to $(2\pi e^2/\kappa q)f(q)$ where $f(q) \leq 1$ is the quasi-2D form factor due to the finite quantum thickness effect [and $f(q) = 1$ in the ideal 2D limit]. Since the modification to the transport theory for $f(q) < 1$ is well-known^{1,28} we do not provide any details, concentrating instead on the numerical results for n_c in the realistic quasi-2D situation.

In Fig. 8 we show our n_c^{IR} and n_c^{per} results [Fig. 8(a)] for n- and p-GaAs quantum wells (using $\tau = \tau_t$ so that $\rho_c^{IR} = h/e^2$). For the purpose of comparison, we also provide our results for the strict 2D limit (i.e., zero quantum well thickness $a = 0$) in Fig. 8(b). For $n_c^{per} = 0.1\sqrt{n_i}/d$, the only effect of finite well-thickness ($a \neq 0$) is that the effective value of ‘ d ’ changes by a , changing n_c^{per} to $n_c^{per} = 0.1\sqrt{n_i}/(d + a/2)$. For n_c^{IR} , the finite thickness increases the effective mean free path l , and thus sup-

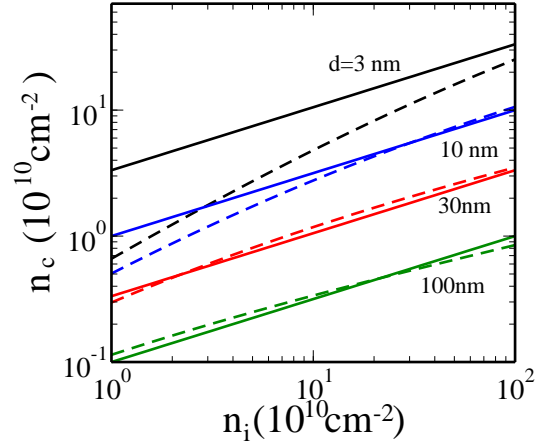


FIG. 9. The calculated critical density of n-MOSFET as a function of impurity density n_i for fixed impurity locations $d = 3, 10, 30, 100$ nm (from top to bottom). Here the finite thickness of quasi-2D system is considered. Solid (dashed) lines represent the percolation critical density, n_c^{per} (Ioffe-Regel critical density, n_c^{IR}).

press the resultant n_c . Thus, both n_c^{IR} and n_c^{per} are suppressed by the finite thickness with this suppression effect being very strong for n_c^{per} when $d < a$. A comparison of Figs. 8(a) and (b) bear this out, and thus the finite thickness effect is only quantitative with the qualitative power law dependence of n_c on n_i being approximately the same.

In Fig. 9 we show our realistic quasi-2D results for n-Si-MOSFETs where the quasi-2D quantum thickness is determined self-consistently by the carrier density n itself¹ which we incorporate through the variational Stern-Howard wavefunction³⁷. We note that for small values of d (which is the expected situation in Si-MOSFETs since the charged impurities are typically in the SiO₂ layer close to the Si-SiO₂ interface), $n_c^{IR} \sim 10^{10} - 10^{11}$ cm⁻² for $n_i \sim 10^{10} - 10^{11}$ cm⁻² whereas $n_c^{IR} > 10^{11}$ cm⁻² for $n_i > 10^{11}$ cm⁻². These findings are consistent with the higher- and lower-mobility Si-MOSFET devices, respectively.

One important qualitative point to note in Figs. 8 and 9 is that while there is a large difference between percolation and Ioffe-Regel predictions for n_c for large values of ‘ d ’, for small values of d , they are virtually indistinguishable. We also note that the materials difference (e.g., n- versus p-GaAs 2D systems in Fig. 8) is rather small with respect to the calculated n_c for the same disorder. It may be worthwhile to point out that writing $n_c \sim n_i^\delta$ in Fig. 9, we get $\delta = \delta(d, n_i)$, and our best numerical estimate for the exponent δ is: $\delta \approx 0.8 - 1$ for $d = 1$ nm, $\delta \approx 0.6 - 0.9$ for $d = 5$ nm, and $\delta \approx 0.5 - 0.8$ for $d = 15$ nm. Since $\mu \sim n_i^{-1}$, we can approximate $\gamma = \delta$ (where $n_c \sim \mu_m^{-\gamma}$), and thus our earlier estimate of $\gamma \approx 0.67$ for Si-MOSFET is consistent with $d = 1 - 2$ nm. This is a stringent consistency check on our theory since, indeed, the random charged impurities in Si MOSFETs are

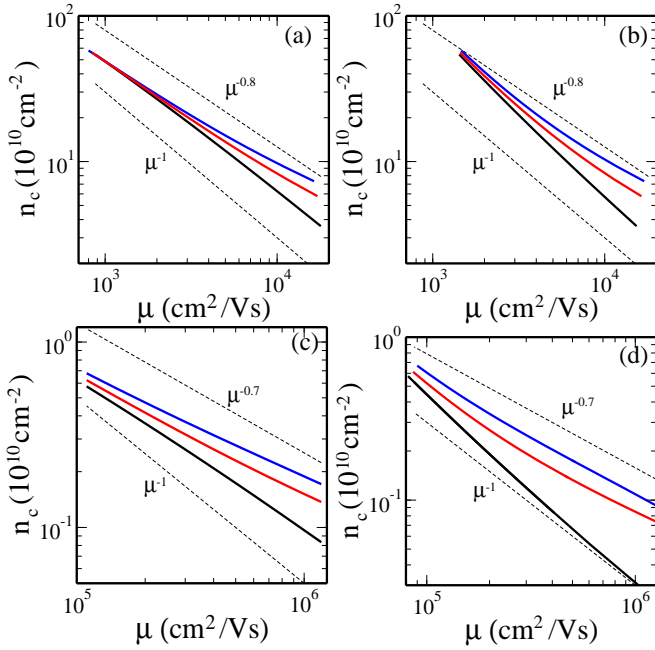


FIG. 10. (a) and (b) show the calculated Ioffe-Regel critical density n_c^{IR} of Si-MOSFET as a function of mobility for different temperatures, $T = 0, 1,$ and 2K (from bottom to top). The mobility is calculated (a) at a given high density $n = 5 \times 10^{11} \text{ cm}^{-2}$ and (b) at $n = 5n_c$. (c) and (d) show the n_c of n-GaAs as a function of mobility for different temperatures, $T = 0, 0.2,$ and 0.5K (from bottom to top). The mobility is calculated (c) at a given high density $n = 5 \times 10^{10} \text{ cm}^{-2}$ and (b) at $n = 5n_c$.

known to be located $1 - 2 \text{ nm}$ inside the oxide layer near the Si-SiO₂ interface.

In Fig. 10 we show our calculated Ioffe-Regel value of n_c as a function of a fiduciary “maximum mobility” defined as the mobility calculated for exactly the same value of disorder parameters (i.e., the same sample), but at a much higher density $n_m \gg n_c$. The precise dependence of n_c on the high-density mobility μ , of course, depends somewhat on the fiduciary density chosen for the high-density mobility, but the basic finding is that the power law (γ) dependence, $n_c \sim \mu_m^{-\gamma}$, is a function of temperature, and typically $\gamma \sim 0.7 - 0.8$ as already pointed out empirically by Sarachik a long time ago²⁶. The fact that $\gamma \approx 0.6 - 0.8$ is consistent with experimental findings in different systems is an indication that the experimental 2D MIT is likely to be a strong localization crossover phenomenon. One salient feature of the results presented in Fig. 10 is that the effective exponent γ , $n_c \sim \mu_m^{-\gamma}$ where μ_m is the mobility at same high density $n_m \gg n_c$, depends strongly on the temperature (as one would expect because of the strong temperature dependence of the 2D metallic resistivity for $n \gtrsim n_c$ provided n_c is not too large).

In Fig. 11 we show our numerically calculated $n_c(T)$, based on the finite-temperature Ioffe-Regel criterion $k_F l(T) = 1$, as a function of temperature. As discussed

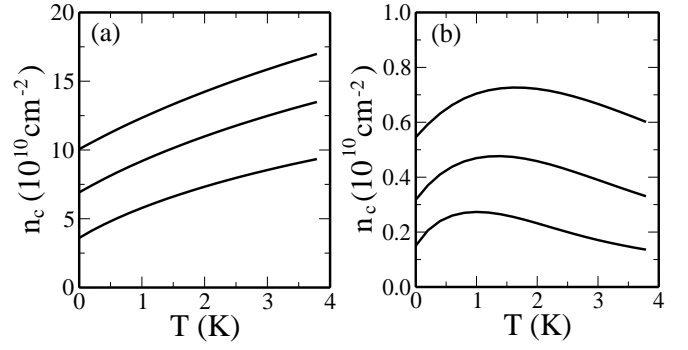


FIG. 11. Calculated Ioffe-Regel $n_c(T)$ of (a) Si-MOSFET as a function of temperature for different impurity densities $n_i = 0.5, 1.0, 1.5 \times 10^{11} \text{ cm}^{-2}$ (from bottom to top) and (b) n-GaAs for $n_i = 0.2, 0.5, 1.0 \times 10^{10} \text{ cm}^{-2}$ (from bottom to top).

earlier, $n_c(T)$ first increases with T and then decreases when $T \lesssim T_F$. However, the overall variation in $n_c(T)$ is less than a factor of 2 in our results. We mention that the results shown in Fig. 11(a) and (b) agree well respectively with the experimentally measured temperature dependence of the critical 2D MIT density in Si MOSFETs¹⁷ and 2D electrons¹⁵ and holes¹⁸ in GaAs systems, providing strong support for our basic Ioffe-Regel model describing the 2D MIT crossover.

In Fig. 12, we show that the calculated maximum mobility dependence of n_c is to some extent dependent on how the maximum mobility is chosen, and thus one cannot really discuss a unique dependence of n_c on the maximum mobility, which is obvious from the fact that both $n_c = n_c(n_i, d)$ and the mobility $\mu = \mu(n_i, d)$ are independent functions of n_i and d . What is interesting, however, is the finding that the exponent γ (with $n_c \sim \mu_m^{-\gamma}$) remains within our analytical finding of $\gamma \approx 0.6 - 0.8$ for a wide range of definitions of the maximum mobility μ .

In Fig. 13 we show how our realistic numerical results change if the quantum mean free path with $l = l_q = v_F \tau_q$ is used in the $k_F l = 1$ criterion for 2D MIT. There is no qualitative change in the results with τ_q replacing τ_t in the Ioffe-Regel criterion as we already emphasized earlier in this paper.

Finally, in Figs 14 and 15 we show the effect of an applied parallel magnetic field B on the critical density $n_c(B)$ due to the spin-polarization-induced lifting of spin degeneracy g_s from $g_s = 2$ at $B = 0$ to $g_s = 1$ at $B = B_s$ where B_s is the applied field strength to fully spin-polarize the 2D electrons. We show numerical results only for Si-MOSFETs here since the qualitative effect of the parallel field on 2D MIT is the same for all 2D systems since the relevant physics is the suppression of screening (and hence suppression of the transport mean free path l) due to the applied magnetic field. We neglect all orbital effects of the applied magnetic field which could enhance $n_c(B)$ even more for systems with large quasi-2D thickness³⁸. As mentioned already, the

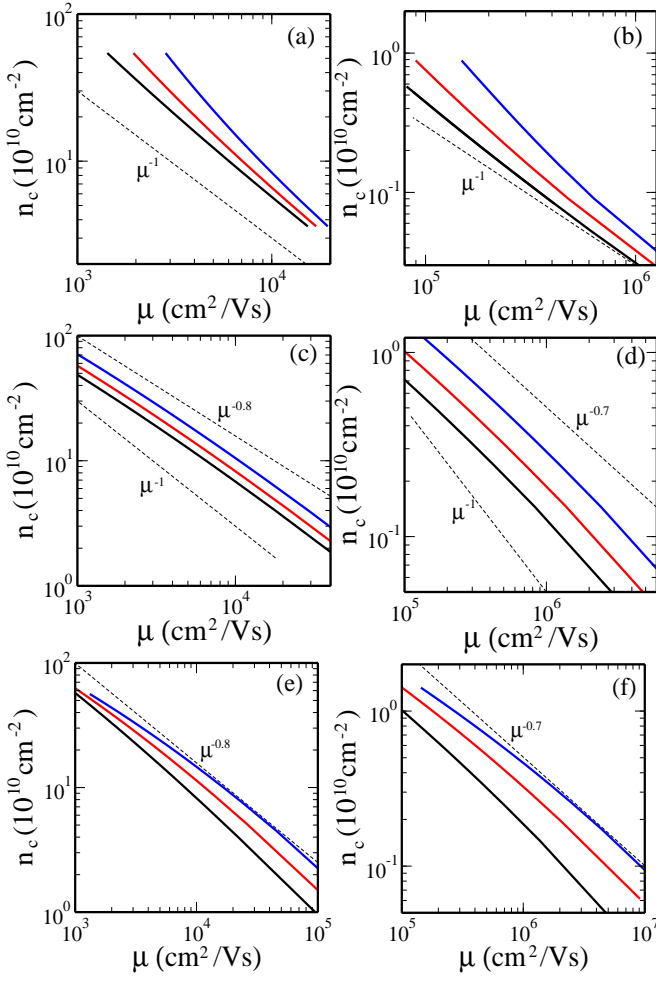


FIG. 12. Calculated zero temperature Ioffe-Regel critical densities (solid lines) as a function of a reference mobility for (a) Si-MOSFET and (b) for n-GaAs. The reference mobility is calculated for different densities $n = 5n_c, 10n_c, 20n_c$ (from bottom to top). Zero temperature n_c as a function of mobility calculated at (c) $n = 5, 10, 20 \times 10^{11} \text{ cm}^{-2}$ (from bottom to top) for Si-MOSFET and (d) $n = 5, 10, 20 \times 10^{10} \text{ cm}^{-2}$ for n-GaAs (from bottom to top). (e) Zero temperature n_c of Si-MOSFET as a function of a reference mobility calculated at $n = 10 \times 10^{11} \text{ cm}^{-2}$ for different locations of impurity center, $d = 0, 10, \text{ and } 20 \text{ \AA}$ (from bottom to top), and (f) n_c of n-GaAs as a function of a mobility at $n = 10 \times 10^{10} \text{ cm}^{-2}$ for different locations of impurity center, $d = 0, 50, \text{ and } 100 \text{ \AA}$ (from bottom to top).

maximum possible effect of the magnetic field is an enhancement of n_c by a factor of $\sqrt{2}$ due to the reduction of spin degeneracy from 2 to 1. Thus, our results in Fig. 14 show an approximate 40% enhancement of n_c in the presence of the applied field at $T = 0$ whereas at finite temperatures the effect is smaller. We emphasize that although the spin-polarization-induced enhancement of $n_c(B)$ compared with its $B = 0$ value is a universal qualitative phenomenon as long as screened Coulomb disorder is the dominant underlying transport scattering mecha-

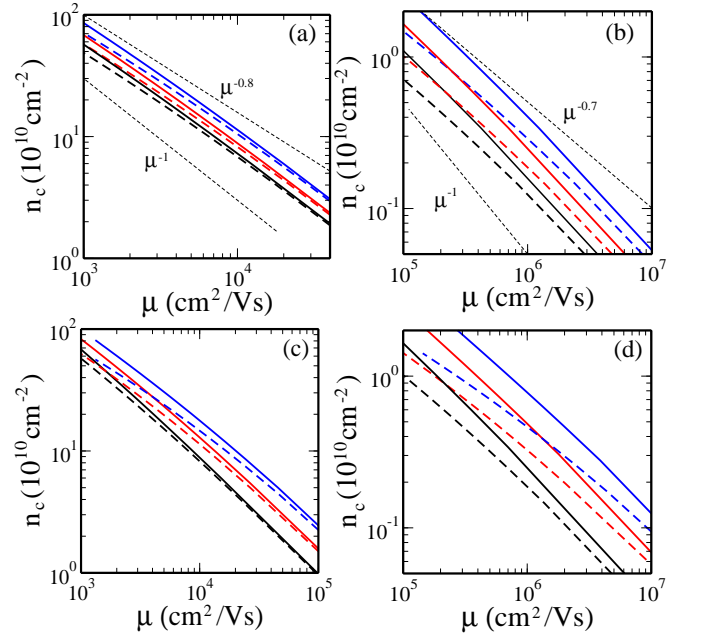


FIG. 13. (a) and (b) show, respectively, the calculated n_c with the quantum mean free path using the same parameters of Fig. 12(c) and (d) where the transport mean free path is used. Solid (dashed) lines indicate the results with quantum (transport) mean free path. (c) and (d) show the calculated n_c with the quantum mean free path using the same parameters of Fig. 12(e) and (f) where the transport mean free path is used, respectively. Solid (dashed) lines indicate the results with quantum (transport) mean free path.

nism, the actual quantitative effect would be miniscule (and experimentally unobservable) if $n_c(B = 0) = n_c$ is very large (as it is highly disordered 2D systems where the 2D MIT phenomena have no dramatic consequences) since $B_s = 2E_c/g\mu_B$ with $E_c = E_F(n = n_c)$ would be very large when n_c is large, and thus $B/B_s \ll 1$ limit would apply on any physically applicable magnetic field in the laboratory making $n_c(B) \approx n_c(B = 0)$. It is only when n_c [and hence $E_c = E_F(n_c)$] is sufficiently small that the applied parallel field induced enhancement of n_c can be experimentally relevant since the available laboratory applied field could reach the $B/B_s \sim 1$ regime. Thus, the condition for the observation of strong temperature dependence of the metallic resistivity and the condition for the observation of strong magnetic field dependence of 2D MIT are closely related as they both require fairly small n_c (and therefore very high-quality 2D samples) so that T/T_F and B/B_s can be relatively large in respective cases. This close connection between the temperature dependence and the magnetic field dependence of 2D MIT phenomena is experimentally well-established, and has already been noted in the literature³¹.

We note that at very low applied field values in Fig. 14, there is a small upturn in the critical density compared with its zero-field value. This is a real effect arising from the increase in effective k_F induced by the applied

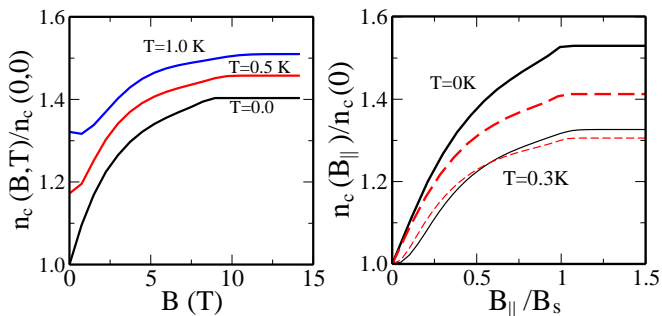


FIG. 14. (a) Calculated $n_c(B)$ as a function of parallel magnetic field B for an impurity density $n_i = 10^{11} \text{ cm}^{-2}$ and for different temperatures $T = 0.0, 0.5, 0.1 \text{ K}$. The critical density is normalized by the critical density calculated at $B = 0$ and $T = 0$, where $n_c(0, 0) = 7 \times 10^{10} \text{ cm}^{-2}$. Above B_s the scattering time τ is constant in this model, which gives the saturation of the critical density. (b) Calculated $n_c(B)$ as a function of parallel magnetic field B_{\parallel} for two different impurity densities [$n_i = 5 \times 10^{10}$ (solid lines) and 10^{11} cm^{-2} (dashed lines)] and for two temperatures [$T = 0\text{K}$ (thick lines) and $T = 0.3\text{K}$ (thin lines)]. The critical density is normalized by the critical density calculated at $B = 0$ and at given temperature, $n_c(0, T)$.

field which always suppresses n_c at finite field compared with its zero-field value, as noted earlier in this paper. If screening effects are unimportant (e.g. scattering by unscreened short-range disorder or at very high carrier density with $2k_F \gg q_{TF}$), then this Fermi surface effect would dominate the finite field transport properties. But the 2D MIT phenomenon occurs at low values of n_c , where $q_{TF} > 2k_F$, and screening effects dominate, leading to a suppression of the metallic phase and an increase of n_c at finite applied magnetic field.

Finally, in Fig. 15 we show our numerical results on the valley-degeneracy dependence of n_c by plotting the numerically calculated $n_c(g_v)$ as a function of the valley degeneracy g_v (at fixed $g_s = 2$) which we assume for this purpose to be a fictitious continuous variable – in reality g_v is 1 or 2 for Si(100)-MOSFETs [whereas for Si(111)-MOSFETs, $g_v = 6$ is allowed]. As expected $n_c(g_v)$ behaves very similarly to the spin-polarization effect on n_c , and with decreasing valley degeneracy, n_c is enhanced since screening is reduced. This dependence of n_c on spin and valley degeneracy of the 2D system is consistent with detailed experimental results reported in 2D ALAs system³². We emphasize that our calculated $n_c(g_s)$ for fixed g_v is identical to results shown in Fig. 15 since both g_s and g_v enter the theory equivalently as the product $g_s g_v$ through the density of states. We mention that for $T \neq 0$ (not shown in Fig. 15), $n_c(g_v)$ softens somewhat showing a weaker dependence of n_c on g_v . The numerical $n_c(g_v)$ in Fig. 15 agrees exactly with the analytical dependence $n_c^{IR} \propto g_v^{-1}$ for $k_F d \ll 1$ which is satisfied essentially for all values of n_c shown in Fig. 15.

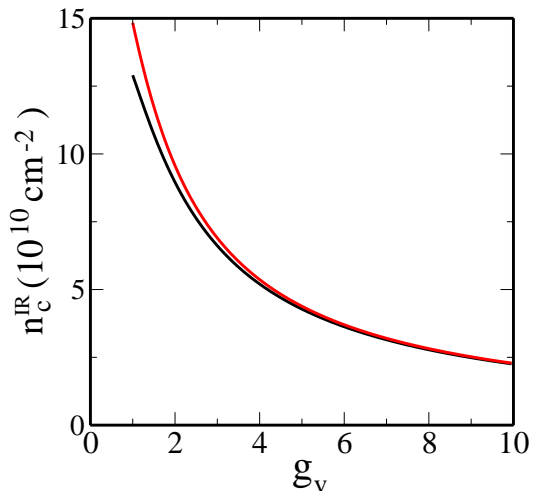


FIG. 15. The calculated Ioffe-Regel critical density of Si-MOSFET as a function of valley degeneracy. Black solid (red dashed) line indicates the n_c^{IR} calculated from the transport (quantum) scattering time τ_t (τ_q). The results are shown for an ideal 2D system with zero thickness and $d = 1 \text{ nm}$ – a finite thickness corresponds to a larger value of effective ‘ d ’, decreasing n_c accordingly.

III. DISCUSSION

We have studied 2D MIT as a strong localization induced crossover phenomenon determined by the Ioffe-Regel criterion (comparing with the corresponding classical percolation transition in the disorder-induced ‘mountains-and-lakes’ inhomogeneous potential fluctuations landscape). There are several distinct aspects of the 2D MIT phenomenology we have addressed in this work theoretically. The main results obtained in this paper involve theoretical and numerical calculations of the crossover critical density n_c^{IR} for 2D MIT using the Ioffe-Regel criterion and its comparison with the corresponding percolation transition density n_c^{per} .

In addition to obtaining n_c , we also provide results for the critical resistivity $\rho_c = \rho(n = n_c)$, which at $T = 0$, is by definition $\rho_c = 2h/(g_s g_v e^2)$. For a percolation transition at $n = n_c^{per} = 0.1 \sqrt{n_i}/d$, in principle, ρ_c^{per} could have any value, but in practice $\rho_c^{per} \sim h/e^2$ seems to apply extensively for realistic 2D sample parameters.

All our theoretical results use a minimal model of Coulomb disorder characterized by a random 2D charged impurity density n_i and a separation of d between the impurities and the 2D carriers. More complex models of disorder are straightforward to include in the theory, but will involve more (than two) free parameters, making it difficult to interpret and understand the theoretical results. Since precise information about the details of disorder is not typically available for high-quality 2D semiconductor systems manifesting 2D MIT, our 2-parameter impurity model is a reasonable starting point for discussing the 2D MIT phenomena.

Below we summarize and critically discuss our impor-

tant findings and related questions focusing on the key features of our theory as compared with the experimental 2D MIT phenomenology.

A. Localization versus percolation

A question of great importance, of course, is whether the 2D MIT at $n \approx n_c$ is a strong localization quantum crossover or classical percolation, i.e., whether $n_c = n_c^{IR}$ or $n_c = n_c^{per}$. At first sight, it appears that our theory should be able to answer this question with sharp precision since the physical origin and the mathematical description of the Ioffe-Regel quantum crossover and the percolation transition are completely distinct. This turns out to be a much more difficult issue than anticipated at first because n_c^{IR} and n_c^{per} have similar magnitudes (both in qualitative agreement with experimental n_c) in many situations for realistic values of sample parameters. This is a rather surprising finding of our work that could not have been anticipated earlier. Even more surprisingly we find that the critical resistivity $\rho_c = \rho(n = n_c)$ is similar for both Ioffe-Regel theory and percolation theory! This is a very unexpected and rather strange result since in principle $\rho_c^{per} = \rho(n = n_c^{per})$ is allowed to be arbitrary whereas ρ_c^{IR} is closely related to the resistance quantum $h/e^2 \approx 25,600\Omega$ since it arises from quantum localization. But our explicit calculations for 2D n-Si, n-GaAs, and p-GaAs systems show that for realistic experimental parameters (with $n_c \sim 10^9 - 10^{11} \text{ cm}^{-2}$), ρ_c values calculated from localization and percolation considerations are not widely different although their dependences on system parameters could be quite different. In view of this similarity between absolute values of n_c (and ρ_c) in the two theories, it is not easy to manifestly choose one mechanism over the other as determining the 2D MIT crossover density n_c , at least using the experimental data on n_c and ρ_c only.

One practical possibility is that as the carrier density is lowered from the high-density metallic phase ($n \gg n_c$) to the low-density insulating phase ($n < n_c$), whichever transition occurs first (i.e., at higher carrier density) in a given sample dominates the actual crossover behavior in that system. (We mention here that our theoretical calculation of n_c and ρ_c explicitly approaches the transition from above, i.e., from the metallic phase.) Thus, $n_c = n_c^{per}$ if $n_c^{per} > n_c^{IR}$ and $n_c = n_c^{IR}$ if $n_c^{IR} > n_c^{per}$. At very low temperatures, however, quantum interference must always be present and therefore $n_c \rightarrow n_c^{IR}$ as $T \rightarrow 0$. Careful experiments should be carried out to investigate this question of whether n_c is better described as localization or as percolation. We emphasize that the experimental finding that $\rho_c \sim h/e^2$ (typically within a factor of 2 – 3) does not automatically imply that n_c is described by n_c^{IR} since our explicit numerical calculations indicate that, perhaps purely coincidentally, $\rho_c \sim h/e^2$ (again within a factor of 2 – 3) is also true for $\rho_c = \rho_c^{per} = \rho(n = n_c^{per})$. We discuss the issue of

localization versus percolation more below in the context of comparing theory and experiment.

There is one particular experimental finding, however, which can only be explained by the quantum Ioffe-Regel theory with the classical percolation theory failing completely. The dependence of n_c on an applied parallel magnetic field, which is widely reported experimentally, can only be explained correctly by the Ioffe-Regel theory and not at all by the percolation theory.

B. Theory and experiment

An important issue is how our theoretically calculated n_c compares with the observed experimental dependence of the critical density on various system parameters such as “maximum” mobility, temperature, external magnetic field, valley degeneracy, effective mass, etc. In this respect (i.e., when compared with experimental findings), the Ioffe-Regel criterion describing 2D MIT as a crossover phenomenon seems to be in much better agreement (both qualitative and quantitative) with observations than the percolation theory. In particular, the fact that the 2D MIT behavior (specifically, the value of n_c itself) depends on an applied parallel magnetic field is difficult to reconcile with the percolation transition which gives a nominally density-independent explicit value of $n_c = n_c^{per} \approx 0.1\sqrt{n_i}/d$. The Ioffe-Regel theory by contrast correctly predicts an increasing n_c with the applied parallel field (i.e., a field-induced suppression of the metallic phase much discussed in the literature^{30,31} on 2D MIT) arising from the spin-polarization of the 2D system. Similarly, the valley degeneracy dependence of n_c (and its equivalence to the spin degeneracy dependence), which has been experimentally demonstrated³², is very naturally explained in the Ioffe-Regel theory as arising from the variation in screening due to the modification in the density of states, whereas it has no explanation within the percolation theory. We see no obvious way of incorporating the applied magnetic field effect in the percolation picture, and thus it appears that 2D MIT, at least for the 2D systems manifesting a strong magnetic field dependence of n_c , is incompatible with the percolation transition.

The most important experimental parameter determining the crossover density n_c is, of course, the sample quality (or disorder) as discussed throughout this article. We emphasize that although n_c obviously increases with increasing disorder, and this is the key reason for the 2D MIT phenomena manifesting itself only in the 1990s when sufficiently high-quality 2D systems could be studied with sufficiently low values of n_c , there does not, in principle, exist a simple relationship between n_c and the sample mobility μ (at a density $n \gg n_c$). The reason for this is that the sample disorder is minimally determined by at least two independent parameters (n_i and d), and therefore it is, in principle, allowed for n_c and μ_m [with $\mu_m = \mu(n = n_m)$ where $n_m \gg n_c$ is some specific high

density] to be completely independent parameters. Thus, in principle, a sample with very high μ_m could have much higher n_c than another sample with low μ_m although it is probably not very likely.

With the above caveat in mind we can, however, obtain from the Ioffe-Regel (or percolation) theory how n_c varies with n_i and d separately, and we can also calculate how the mobility $\mu(n)$ varies with n_i and d as well as carrier density n .²⁵ Therefore, the disorder dependence of n_c is completely specified in our theory through the two disorder parameters n_i and d . Assuming a fixed d , we can convert the n_i -dependence of n_c to an effective dependence on the mobility at some high carrier density, finding, $n_c \sim \mu_m^{-0.7}$ in the Ioffe-Regel theory and $n_c \sim \mu_m^{-0.5}$ in the percolation theory. The fact that Sarachik already pointed out more than 10 years ago²⁶ an empirical relationship, $n_c \sim \mu_m^{-0.7}$, which is in agreement with the Ioffe-Regel theory, is a strong agreement in favor of the Ioffe-Regel theory.

Assuming $k_F d \ll 1$, we obtain theoretically $I_c^{IR} \sim n_i d^0$ and $n_c^{per} \sim n_i d^{-1/2}$ whereas for $k_F d \gg 1$, $n_c^{IR} \sim (n_i/d)^{2/3}$ and $n_c^{per} \sim (n_i/d)^{1/2}$. In principle, these asymptotic dependence on n_i and d can be explicitly checked experimentally, but we know of no detailed experimental study of the critical density on the microscopic parameters defining the disorder.

At this stage, the most convincing agreement between our theory for n_c and experiment comes from (1) $n_c^{IR} \sim \mu_m^{-0.67}$ type behavior noted earlier empirically²⁶; (2) the parallel field induced enhancement of n_c^{IR} ;^{30,31} (3) the dependence of n_c^{IR} on the valley degeneracy and its equivalence to the spin-degeneracy dependence³². We note that all three properties mentioned here favor the 2D MIT being a strong localization induced crossover phenomenon as determined by the Ioffe-Regel criterion (in contrast to the classical percolation transition). In this context, we must mention one small (but significant) remaining discrepancy between the Ioffe-Regel theory and the experimental finding on 2D MIT. The Ioffe-Regel theory predicts that the critical resistivity $\rho_c = \rho(n_c)$ at the transition must necessarily obey the inequality

$$\rho_c^{IR} \leq \frac{h}{e^2} \frac{2}{g_s g_v}, \quad (44)$$

which means that even if the spin and valley degeneracy are lifted $\rho_c < h/e^2 \approx 25,6000\Omega$. Experimentally, this inequality is obeyed almost universally with the most important exception being the original Si-MOSFET data of Kravchenko *et al.* who consistently found $\rho_c^{Si} \approx 1.5h/e^2$. We have no way of explaining $\rho_c > h/e^2$ (at least at $T = 0$) within the Ioffe-Regel theory. One possibility is that $\rho_c > h/e^2$ is a finite temperature effect, and $\rho_c(T \rightarrow 0)$ approaches h/e^2 , but we simply do not know if this is true or not. We emphasize, however, that the vast majority of 2D MIT data are consistent with ρ_c values obtained from the Ioffe-Regel theory, and thus the critical resistivity issue may not be a particularly important problem for the Ioffe-Regel theory, particularly since the

extrapolated value of $\rho_c(T \rightarrow 0)$ is not easy to ascertain experimentally from finite temperature transport measurements.

C. Transition versus crossover

We have studied the 2D MIT as a crossover in this work (either described by Ioffe-Regel criterion or by percolation), not as a true localization quantum phase transition since two is established to be the lower critical dimensions for the Anderson localization phenomenon³⁹, both for noninteracting electrons in a disordered system^{7,40} and in the presence of disorder and interaction⁴¹. We consider the metallic phase (for $n > n_c$) to be an effective metal which at $T = 0$ will be insulating in an infinite system. The metal-to-insulator crossover in our theory arises from the strong modification in the effective screened Coulomb disorder which becomes very strong as the carrier density is lowered, leading to the $k_F l = 1$ condition defining the MIT crossover point. The fact that our calculated n_c is in qualitative agreement with experimental observations is persuasive evidence in support of 2D MIT being a crossover phenomenon, but our theory can shed no light on the theoretical question of whether quantum criticality in playing a role in this problem or not. In particular, we emphasize that we have no way of ruling out the 2D MIT as a true quantum phase transition since this issue is simply beyond the scope of our work, which treats the problem manifestly as a crossover phenomenon described by the Ioffe-Regel criterion.

IV. CONCLUSION

Assuming 2D MIT to be a crossover phenomenon from a weakly localized effective metallic phase to a strongly localized insulating state, we have developed a theory for the critical density for the transition from the higher-density effective metallic phase to the lower-density strongly localized insulating phase. The calculated critical density based on the well-known Ioffe-Regel criterion for strong localization is in qualitative agreement with experimental observations on 2D MIT with respect to its dependence on disorder, applied parallel magnetic field, valley degeneracy, and materials parameters.

Our main findings are the following: (1) The critical density n_c for the 2D MIT crossover varies with the maximum sample mobility μ_m (measured at some high carrier density $n \gg n_c$) according to the approximate scaling law, $n_c \sim \mu_m^{-\gamma}$, with the exponent $\gamma \approx 0.7$ (for screened Coulomb disorder) and 1 (for purely zero-range δ -function disorder) as derived from the Ioffe-Regel criterion and $\gamma = 0.5$ (for all disorder) as derived from the semiclassical percolation theory. (2) The Ioffe-Regel criterion predicts an enhancement of n_c with decreasing spin-degeneracy, as, for example, in the presence of an

applied parallel magnetic field inducing spin-polarization in the system provided that the critical density n_c is fairly low at zero spin-polarization (so that the condition $q_{TF} \gtrsim 2k_F$ or $q_{TF} \gg 2k_F$ is satisfied). By contrast, the percolation theory predicts no dependence of n_c on the spin degeneracy. (3) The Ioffe-Regel criterion predicts an enhancement of n_c with decreasing valley degeneracy in the system as, for example, could be induced by applying a suitable external strain. In fact, the Ioffe-Regel criterion predicts that the dependence of the critical density $n_c(g_s, g_v)$ on the spin- and valley-degeneracy to be approximately equivalent, i.e., increasing (decreasing) g_s or g_v decreases (increases) n_c if all other parameters are fixed. This mutually equivalent spin and valley-degeneracy dependence of n_c arises from the 2D screening being dependent on g_s and g_v equivalently since the density of states is proportional to $g_s g_v$. One direct prediction of the Ioffe-Regel theory is thus that the most metallic (insulating) situation will manifest itself for the largest (smallest) values of the product $g_s g_v$, and therefore, n_c will be the smallest (largest) for the largest (smallest) values of $g_s g_v$ in the system. The percolation theory predicts the 2D MIT phenomena to be completely independent of g_s and/or g_v , and thus does not in any way predict any dependence of n_c on spin- or valley-polarization. We mention that all three of these theoretical findings based on the Ioffe-Regel criterion are in good qualitative and semiquantitative agreement with experimental results on 2D MIT whereas the predictions of the percolation theory – in particular, the $n_c \propto \sqrt{\mu_m}$ dependence and the lack of dependence of n_c on g_s and g_v – are in disagreement with the empirical evidence.

In addition to the above qualitative physical results following directly from our theory, we also find that the actual quantitative values of n_c calculated on the basis of the Ioffe-Regel criterion to be consistent with the experimental results. In particular, we find that the Ioffe-Regel criterion gives the following approximate critical density values for typical high-mobility 2D systems studied in the existing 2D MIT literature²⁻⁶: $n_c \approx 10^{11} \text{ cm}^{-2}$ (for Si MOSFETs); 10^{10} cm^{-2} (for p-GaAs); 10^9 cm^{-2} (for n-GaAs). By contrast, we find that the lower-quality Si MOSFETs studied extensively during the 1970s and early 1980s¹ should typically have $n_c \approx 10^{12} \text{ cm}^{-2}$ according to the Ioffe-Regel criterion. This high value of n_c , with a corresponding Fermi temperature $\sim 73 \text{ K}$, is not only consistent with the experimental n_c values found in older MOSFETs¹ with lower values of maximum mobility ($\mu_m < 5000 \text{ cm}^2/\text{Vs}$), but also provides an obvious explanation for why the 2D MIT phenomenon could only be observed after very high mobility ($\mu_m \gtrsim 20,000 \text{ cm}^2/\text{Vs}$) Si MOS samples become available in the 1990s.²² A high value of n_c with a concomitant high value of Fermi temperature makes it impossible²⁸ for the 2D effective metallic phase (for $n > n_c$) to manifest any temperature dependence in its resistivity arising purely from an electronic mechanism.

Several open questions remain for future investiga-

tions. Although our main conclusion is that the 2D MIT (at least at very low temperatures) is strong-localization induced crossover phenomenon as constrained by an Ioffe-Regel type quantum interference condition, the role of percolation in the inhomogeneous potential fluctuation landscape in affecting the crossover behavior remains unclear. For Si-MOSFETs, where the random charged impurities are located at the Si-SiO₂ interface close to the 2D electron system, it is hard to see how and why percolation could be relevant, but in modulation-doped GaAs structures, where the dopants are far away from the electrons, percolation could conceivably be relevant. One possibility we have speculated about is that the transition itself crosses over from being percolation like at higher temperatures to being Ioffe-Regel-like at lower temperatures as quantum tunneling and quantum interference become effective. But these are all mere speculations, and we do not have a theory combining percolation and strong localization crossover, which remains an important open issue in the long-range fluctuating potential landscape of Coulomb disorder. In the current work, we have only compared localization and percolation crossovers as distinct physical processes, concluding that the experimental observations are more consistent with the Ioffe-Regel localization crossover.

Another open question (and an important shortcoming of our theory) is that the theory developed in this paper approaches the transition (i.e., the crossover) from the higher-density effective metallic side (with decreasing density to approach the transition) using Boltzmann transport theory to treat the screened disorder induced carrier scattering. An equivalent theory from the lower-density insulating side (with increasing density to approach the transition) is highly desirable, but is out of scope for our work, and in fact, there is no good idea in the literature about how to approach the transition from the insulating side where the whole concept of a quantum mean free path becomes inapplicable (and therefore the Ioffe-Regel criterion is useless). Such a theory from the insulating side, if available, could be a compelling consistency check for the calculated critical density if the same crossover point is reached theoretically from either direction.

Another issue with our theory, in spite of its good qualitative agreement with essentially all aspects of 2D MIT phenomenology, is that our calculated critical resistivity (i.e., the 2D resistance at the crossover critical density) is only in approximate quantitative agreement with experiments. This may not be a serious problem since the crossover nature of the transition makes it problematic to define a unique zero-temperature critical resistivity (particularly since the 2D resistivity is strongly temperature dependent around the critical density), and it is likely that a proper extrapolation of the experimental data to zero temperature would be in reasonable agreement with our theory since the disagreement is mainly in Si-MOSFETs and is by less than a factor of two. More experimental work is necessary to settle the question for

the precise value of the $T = 0$ critical resistivity in 2D MIT in various systems.

Our theory provides a good qualitative explanation for the dependence of the critical density on disorder, applied parallel magnetic field, spin and valley degeneracy, and materials parameters indicating that the Ioffe-Regel criterion, in all likelihood, captures the essential features of the transition between the high-density effective (weakly localized) metallic phase and the low-density strongly localized insulating phase in 2D semiconductors. The issue of whether 2D MIT is or is not a true $T = 0$ quantum phase transition as well as whether or how electron-electron interaction⁴¹ beyond screening affects the transition, however, still remaining open as a theoretical question for future work. What we have established in this work through extensive calculations is that the application of the empirical Ioffe-Regel criterion, which is often used in the literature for a semi-quantitative description of the Anderson localization transition in three-

dimensional systems, to the phenomenon of the apparent two-dimensional metal-insulator transition provides a critical density which agrees well with existing experiments in describing the characteristic dependence of the critical density on disorder, mobility, temperature, and magnetic field, indicating that the observed 2D MIT phenomenon is likely to be a crossover between a weakly localized 2D metal and a strongly localized Anderson insulator.

ACKNOWLEDGEMENTS

This work is supported by LPS-CMTC and Basic Science Research Program through the National Research Foundation of Korea Grant funded by the Ministry of Science, ICT & Future Planning (2009-0083540).

-
- ¹ T. Ando, A. B. Fowler, and F. Stern, *Rev. Mod. Phys.* **54**, 437 (1982).
- ² E. Abrahams, S. V. Kravchenko, and M. P. Sarachik, *Rev. Mod. Phys.* **73**, 251 (2001).
- ³ S. V. Kravchenko, and M. P. Sarachik, *Rep. Prog. Phys.* **67**, 1 (2004).
- ⁴ S. Das Sarma and E. H. Hwang, *Solid State Commun.* **135**, 579 (2005).
- ⁵ B. Spivak, S. V. Kravchenko, S. A. Kivelson, and X. P. A. Gao, *Rev. Mod. Phys.* **82**, 1743 (2010).
- ⁶ S. Das Sarma, S. Adam, E. H. Hwang, and E. Rossi, *Rev. Mod. Phys.* **83**, 407 (2011).
- ⁷ E. Abrahams, P. W. Anderson, D. C. Licciardello, and T. V. Ramakrishnan, *Phys. Rev. Lett.* **42**, 673 (1979).
- ⁸ N. F. Mott, *J. Phys. C* **8**, L239 (1975).
- ⁹ C. J. Adkins, *J. Phys. C* **11**, 851 (1978).
- ¹⁰ D. J. Bishop, D. C. Tsui, and R. C. Dynes, *Phys. Rev. Lett.* **44**, 1153 (1980); F. W. Van Keuls, H. Mathur, H. W. Jiang, and A. J. Dahm *Phys. Rev. B* **56**, 13263 (1997); T. M. Lu, W. Pan, D. C. Tsui, P. C. Liu, Z. Zhang, and Y. H. Xie, *Phys. Rev. Lett.* **107**, 126403 (2011); G. M. Minkov, A. V. Germanenko, O. E. Rut, A. A. Sherstobitov, and B. N. Zvonkov, *Phys. Rev. B* **75**, 235316 (2007); G. M. Minkov, O. E. Rut, A. V. Germanenko, A. A. Sherstobitov, B. N. Zvonkov, E. A. Uskova, and A. A. Birukov, *Phys. Rev. B* **65**, 235322 (2002).
- ¹¹ Patrick A. Lee and T. V. Ramakrishnan, *Rev. Mod. Phys.* **57**, 287 (1985); G. Bergman, *Phys. Rep.* **107**, 1 (1984); C. W. J. Beenakker and H. Van Houten, in *Solid State Physics*, edited by H. Ehrenreich and D. Turnbull (Academic, San Diego, 1991), Vol. **44**.
- ¹² T. M. Klapwijk and S. Das Sarma, *Solid State Commun.* **110**, 581 (1999).
- ¹³ E. H. Hwang and S. Das Sarma, *Phys. Rev. B* **77**, 235437 (2008).
- ¹⁴ A. Lewalle, M. Pepper, C. J. B. Ford, E. H. Hwang, S. Das Sarma, D. J. Paul, and G. Redmond, *Phys. Rev. B* **66** 075324 (2002).
- ¹⁵ M. P. Lilly, J. L. Reno, J. A. Simmons, I. B. Spielman, J. P. Eisenstein, L. N. Pfeiffer, K. W. West, E. H. Hwang, and S. Das Sarma, *Phys. Rev. Lett.* **90**, 056806 (2003).
- ¹⁶ V. Senz, T. Ihn, T. Heinzel, K. Ensslin, G. Dehlinger, D. Grutzmacher, U. Gennser, E. H. Hwang, and S. Das Sarma, *Physica E* **13**, 723 (2002).
- ¹⁷ L. A. Tracy, E. H. Hwang, K. Eng, G. A. Ten Eyck, E. P. Nordberg, K. Childs, M. S. Carroll, M. P. Lilly, and S. Das Sarma, *Phys. Rev. B* **79**, 235307 (2009).
- ¹⁸ M. J. Manfra, E. H. Hwang, S. Das Sarma, L. N. Pfeiffer, K. W. West, and A. M. Sergent, *Phys. Rev. Lett.* **99**, 236402 (2007).
- ¹⁹ H. Noh, M. P. Lilly, D. C. Tsui, J. A. Simmons, E. H. Hwang, S. Das Sarma, L. N. Pfeiffer, and K. W. West, *Phys. Rev. B* **68**, 165308 (2003).
- ²⁰ Q. Li, E. H. Hwang, E. Rossi, and S. Das Sarma *Phys. Rev. Lett.* **107**, 156601 (2011).
- ²¹ K. Eng, R. N. McFarland, and B. E. Kane, *Appl. Phys. Lett.* **87**, 052106 (2005); *Physica E* **34**, 701 (2006); K. Eng, R. N. McFarland, and B. E. Kane, *Phys. Rev. Lett.* **99**, 016801 (2007); B. Hu, T. M. Kott, R. McFarland, and B. E. Kane, *Appl. Phys. Lett.* **100**, 252107 (2012).
- ²² S. V. Kravchenko, G. V. Kravchenko, J. E. Furneaux, V. M. Pudalov, and M. D'Iorio, *Phys. Rev. B* **50**, 8039 (1994); S. V. Kravchenko, W. E. Mason, G. E. Bowker, J. E. Furneaux, V. M. Pudalov, and M. D'Iorio, *Phys. Rev. B* **51**, 7038 (1995); S. V. Kravchenko, W. Mason, J. E. Furneaux, and V. M. Pudalov, *Phys. Rev. Lett.* **75**, 910 (1995); S. V. Kravchenko, M. P. Sarachik, and D. Simonian, *Phys. Rev. Lett.* **83**, 2091 (1999).
- ²³ M. R. Graham, C. J. Adkins, H. Behar, and R. Rosenbaum, *J. Phys.: Condens. Matter* **10**, 809 (1989).
- ²⁴ S. Das Sarma and F. Stern, *Phys. Rev. B* **32**, 8442 (1985).
- ²⁵ S. Das Sarma and E. H. Hwang, *Phys. Rev. B* **88**, 035439 (2013).
- ²⁶ M. P. Sarachik, *Europhys. Lett.* **57** 546 (2002).
- ²⁷ S. Das Sarma and E. H. Hwang, *Phys. Rev. B* **68**, 195315 (2003).

- ²⁸ S. Das Sarma and E. H. Hwang, Phys. Rev. B **69**, 195305 (2004); Phys. Rev. Lett., **83**, 164 (1999).
- ²⁹ S. Das Sarma, M. P. Lilly, E. H. Hwang, L. N. Pfeiffer, K. W. West, and J. L. Reno, Phys. Rev. Lett. **94**, 136401 (2005).
- ³⁰ D. Simonian, S. V. Kravchenko, M.P. Sarachik, and V. M. Pudalov, Phys. Rev. Lett. **79**, 2304 (1997); T. Okamoto, K. Hosoya, S. Kawaji, and A. Yagi, Phys. Rev. Lett. **82**, 3875 (1999); K. M. Mertes, D. Simonian, M. P. Sarachik, S. V. Kravchenko, and T. M. Klapwijk, Phys. Rev. B **60**, R5093 (1999); J. Yoon, C. C. Li, D. Shahar, D. C. Tsui, and M. Shayegan, Phys. Rev. Lett. **84**, 4421 (2000); S. J. Papadakis, E. P. De Poortere, M. Shayegan, and R. Winkler, Phys. Rev. Lett., **84** (2000), p. 5592 (2000); J. Zhu, H. L. Stormer, L. N. Pfeiffer, K. W. Baldwin, and K. W. West, Phys. Rev. Lett. **90**, 056805 (2003).
- ³¹ S. Das Sarma and E. H. Hwang, Phys. Rev. B **72**, 035311 (2005); Phys. Rev. B **72**, 205303, (2005); V. T. Dolgoplov and A. Gold, JETP Lett. **71**, 27 (2000); I. F. Herbut, Phys. Rev. B **63**, 113102 (2001).
- ³² O. Gunawan, T. Gokmen, K. Vakili, M. Padmanabhan, E. P. De Poortere, and M. Shayegan, Nature Phys. **3**, 388 (2007).
- ³³ S. Das Sarma, E. H. Hwang, and Qiuzi Li, Phys. Rev. B **88**, 155310 (2013).
- ³⁴ M. M. Fogler, Phys. Rev. B **69**, 121409 (2004); J. A. Nixon and J. H. Davies, Phys. Rev. B **41**, 7929 (1990); Y. Meir, Phys. Rev. B **61**, 16470 (2000); J. Shi and X. C. Xie, Phys. Rev. Lett. **88**, 086401 (2002); J. Shi, S. He, and X. C. Xie, Phys. Rev. B **60**, R13950 (1999).
- ³⁵ F. G. Pikus and A. L. Efros, Zh. Éksp. Teor. Fiz. **96**, 985 (1989) [Sov. Phys. JETP **69**, 558 (1989)]; A. L. Efros, Solid State Commun. **67**, 1019 (1988).
- ³⁶ A. L. Efros, F. G. Pikus, and V. G. Burnett, Phys. Rev. B **47**, 2233 (1993).
- ³⁷ F. Stern and S. Das Sarma, Phys. Rev. B **30**, 840 (1984); W. E. Howard and F. F. Fang, Phys. Rev. B **13**, 2519 (1976).
- ³⁸ S. Das Sarma and E. H. Hwang, Phys. Rev. Lett. **84**, 5596 (2000).
- ³⁹ D. Belitz and T. R. Kirkpatrick, Rev. Mod. Phys. **66**, 261 (1994); D. Belitz, T. R. Kirkpatrick, and T. Vojta, Rev. Mod. Phys. **77**, 579 (2005).
- ⁴⁰ F. J. Wegner, Z. Phys. B **35**, 207 (1979).
- ⁴¹ A. M. Finkel'stein, Zh. Eksp. Teor. Fiz. **86**, 367 (1984) [Sov. Phys. JETP **59**, 212 (1984)]; Pis'ma Zh. Eksp. Teor. Fiz. **40**, 63 (1984) [JETP Lett. **40**, 796 (1984)]; A. Punnoose and A. M. Finkel'stein, Science **310**, 289 (2005); G. Zala, B. N. Narozhny, and I. L. Aleiner, Phys. Rev. B **64**, 214204 (2001).